Dynamics of upper tropospheric stationary wave anomalies induced by ENSO during the northern summer: A GCM study

R KRISHNAN, C VENKATESAN and R N KESHAVAMURTY

Climate and Global Modelling Division, Indian Institute of Tropical Meteorology, Pune 411 008, India

Ensemble seasonal integrations are carried out with the COLA GCM, with a view to understand the dynamical connection between warm SST anomalies in the equatorial central-eastern Pacific Ocean and the upper level stationary wave anomalies seen during drought years over the Indian summer monsoon region. In addition, experiments with and without orography are performed in order to examine the role of the Himalayas in modulating the El Niño induced stationary wave anomalies over the summer monsoon region.

The GCM simulations show a statistically significant weakening of the summer monsoon activity over India in response to the SST forcing in the equatorial Pacific Ocean. This weakening of the summer monsoon appears to be largely related to modifications of the local Hadley and Walker cells over the summer monsoon region. In addition, it is seen that the anomalous ENSO divergent forcing over the tropical Pacific Ocean can act as a potential source for Rossby wave dispersion. Here one finds the possibility of meridionally propagating Rossby waves, which emanate from the ENSO forcing region, to interact with the subtropical westerlies and generate anomalous highs and lows in the subtropics and extratropics. The quasi-stationary perturbations seen over west Asia, Pakistan and northwest India during drought years, seem to be generated by the above mechanism. An alternate mechanism that could be important for the persistence of the quasi-stationary perturbations seems to be based on the dynamic excitation of middle latitude normal modes which can extract energy from the zonally varying unstable basic flow.

It is seen from the GCM simulations, that the Himalayan orography plays a crucial role in anchoring the El Niño induced extratropical westerly troughs far to the west in the high latitude belt. In the absence of orography it is seen that the ENSO induced extra-tropical cyclonic anomalies tend to intrude southward into the monsoon region thereby destroying the regional scale circulations completely. Another effect due to the Himalayas is to generate lee waves on the eastern side of the topographic barrier which encircle the globe in the subtropics and midlatitudes.

1. Introduction

1.1 *Observational aspects*

The works of Keshavamurty and Awade (1974); Joseph (1978); Keshavamurty *et al* (1980); Joseph *et al* (1981); Verma (1982); and Rajeevan (1991, 1993)) indicate the occurrence of prominent circulation and thermal anomalies in the upper troposphere over north India and the neighbourhood during drought years. It is seen that these signals manifest in the form of well-defined cold cyclonic circulation anomalies in the upper troposphere. The quasi-stationary anomalies generally have a long persistence and indications of these anomalous signals can be traced right from the previous winter months (Joseph 1978). The persistence of such quasi-stationary features tends to inhibit the development of the upper

Keywords. Stationary wave anomalies; ENSO; Rossby wave dispersion; Indian summer monsoon.

Proc. Indian Acad. Sci. (Earth Planet. Sci.), **107**, No. 1, March 1998, pp. 65–90

tropospheric anticyclones and the Tropical Easterly Jet (TEJ). Moreover the presence of cold air over the northern parts of India reduces the meridional thermal contrast over the subcontinent. The above dynamical abnormalities produce an adverse effect on the summer monsoon activity over India (Keshavamurty and Awade (1974)).

Ramaswamy (1958, 1962) examined the general circulation at 500 hPa in a global perspective and inferred that breaks in the Indian summer monsoon were related to large amplitude Rossby waves associated with the mid-latitude systems. Pisharoty and Desai (1956) and Mooley (1957) studied the effect of mid-latitude westerly systems on Indian monsoon and found that the intrusion of these waves into Indian latitudes either intensify the monsoon in the northern part (Changraney 1966) or can lead to a break monsoon condition. Unni Nayar and Murakami (1978) examined the NMC data for the monsoon period and found that the break monsoon situation was associated with large amplitude Rossby regime in the mid latitudes which resulted in a bifurcation of the Tibetan anticyclone into two parts. Sikka and Grossman (1981) and Bedi *et al* (1981) studied the MONEX data and found that the mid-latitude systems bring very cold air with them and tend to be more active during weak monsoon years. Raman and Rao (1981) observed Asian blocking ridges during weak monsoon conditions. They noted that the mid-latitude troughs preferably tend to stagnate either to the west of 90°E or to the east of 115°E and an east Asian blocking ridge gets stationed in between 90°E and 115°E.

White (1982) carried out an extensive diagnostic study of both stationary and transient waves over the globe for the northern hemispheric summer. Using data from National Meteorological Center (NMC) operational analyses, he described the three dimensional structure of the summertime stationary wave patterns. He identified two distinct stationary wave patterns; one over the sub-tropical monsoon region and the other in the extra-tropics. He noted that the former regime was *global scale* and *monsoonal* (which refers to a baroclinic structure because of the opposite polarity of the tropical circulation between the upper and lower troposphere) while the latter was associated with smaller scales having an equivalent barotropic vertical structure. He attributed the subtropical pattern largely to monsoonal diabatic heating which can be confirmed from the studies of Krishnamurti (1971a); Webster (1972); Murakami (1974) and Gill (1980). White (1982) also pointed out that the summertime mid-latitude patterns resulted from a highly complex and nonlinear response to thermal and orographic forcings.

Studies by Sikka (1980); Bhalme and Mooley (1980); Pant and Parthasarathy (1981); Rasmusson and Carpenter (1983); Rasmusson and Wallace (1983); Shukla and Paolino (1983); Bhalme and Jadhav (1984); Ropelewski and Halpert (1987); Parthasarathy *et al* (1988) and several others, suggest the existence of a negative correlation between the Indian summer monsoon rainfall and ENSO. In keeping with the fact that a majority of bad monsoon years were associated with El Niño events in the equatorial Pacific Ocean, one is prompted to understand the possible dynamical influence of ENSO in generating stationary wave anomalies as seen during years of weak Indian summer monsoon. Although there have been some recent attempts to explore the physical relationship between the two (see, Webster and Yang (1992); and Nigam (1994)), the dynamics of the ENSO-monsoon connection is not adequately clear at the moment.

1.2 *Theoretical and modelling studies of the stationary wave anomalies*

The studies of Bjerknes (1969) and Wright (1977) provided a strong physical basis that warm SST anomalies in the tropical Pacific Ocean can induce anomalous effects on the atmospheric circulation and precipitation patterns at remote locations through teleconnection mechanisms. Atmospheric teleconnections linking tropical convection and extratropical circulations are reasonably well known for the winter months (Wallace and Gutzler (1981); Horel and Wallace (1981); Horel (1981); Van Loon and Madden (1981)). For instance, Horel and Wallace (1981) have documented the link between the equatorial SST anomalies and the Pacific North American (PNA) pattern during the northern winter. Likewise, Van Loon and Madden (1981) presented global relationships of the SO in the northern winter with sea level pressures and temperatures.

With the advent of global data sets and advances in the field of numerical modelling using powerful computers, the interconnection between ENSO and a wide variety of extratropical circulation anomalies is becoming increasingly clear. The early numerical simulations of Rowntree (1972) gave support to Bjerknes (1966, 1969) observational hypothesis that equatorial SST anomalies can produce large changes in the mean tropical Hadley circulation. However a majority of theoretical studies in the past have largely concentrated on establishing dynamical links between wintertime extratropical circulations and convection anomalies in the tropics. So far there have been relatively very few theoretical studies on the summertime teleconnection mechanisms. In a GCM study, Shukla (1975) showed that a decrease of SST between 1–3°C over an area in the Arabian Sea produced a statistically significant reduction of more than 40% rainfall over India. Washington *et al* (1977) examined the sensitivity of the Indian summer monsoon to SST anomalies over the Indian Ocean and Arabian Sea using the NCAR GCM. They noted that although the

Indian Ocean and Arabian Sea SSTs did influence the monsoon rainfall over India, the model simulated rainfall anomalies over the Indian subcontinent were not substantial or statistically significant. Keshavamurty (1982) examined the impact of equatorial Pacific SST anomalies on the atmosphere using the Geophysical Fluid Dynamics Laboratory (GFDL) GCM. He placed a warm idealized SST anomaly of 3°C amplitude over the eastern, central and western Pacific Ocean in three different simulation experiments. His study showed that SST anomalies over the central and eastern equatorial Pacific Oceans were quite efficient in producing a weakening of the summer monsoon over India. The ENSO induced weakening of the Indian summer monsoon seen in his GCM simulations were found to be statistically significant. The results of his simulation experiments were in conformity with the observational analysis by Pan (1979) during the 1972 El Niño. He also noted that the atmospheric response locally over the region of Pacific heating resulted in an anomalous upper level anticyclonic couplet to the north and south of equator which was theoretically consistent with the findings of Gill (1980).

Recent improvements in physics parameterization in GCMs (e.g. Miller *et al* 1992; Sud and Walker 1992) have prompted a renewed effort in monsoon numerical studies using GCMs. A number of serious attempts have been made, in the last few years, to simulate the Indian summer monsoon (e.g. Brankovic *et al* 1993; Fennessy *et al* 1994; Shukla and Fennessy 1994), and also its interannual variability (IAV) (e.g. Palmer *et al* 1992; Zwiers 1993; Sperber *et al* 1994; Chen and Yen 1994; Nigam 1994; Ju and Slingo 1995; Krishnan and Fennessy 1997). Despite the numerous modelling attempts, the dynamics of summertime teleconnections associated with the IAV of the Indian summer monsoon is still not adequately understood at present.

2. Anomalous features during weak monsoons revealed from NCEP/NCAR reanalysis

We shall first carry out a diagnostic examination of the upper tropospheric anomalies during weak summer monsoons using the 13 year (1982–94) NCEP/NCAR reanalysis data (see Kalnay et al (1996)). Since the Indian summer monsoon activity is concentrated during the four months of June to September, we have focussed our study on the JJAS mean values of the global fields. The JJAS climatological (CLIM) values obtained for the thirteen years (1982–1994) are chosen to represent the normal summer monsoon. For the purpose of making anomaly composites, we have classified the 3 years (1982, 1986, 1987) as weak monsoon (WEAK-ISM) years. The summer monsoon rainfall over India was less than 10% below normal during the above years (see Parthasarathy *et al* (1995)). In addition to being weak monsoon years, the WEAK-ISM composite of summertime SST showed warm anomalies in the tropical central-eastern Pacific Ocean. It must be mentioned that the summers of 1982 and 1987 were characterized by the El Niño related positive SST anomalies in the tropical central-eastern Pacific Ocean. However the warm Pacific SST anomalies during JJAS 1986 were rather weak and were seen mostly in the central Pacific Ocean.

2.1 *Rainfall distribution*

Consistent ENSO-precipitation global teleconnnections have been well documented in the past by Stoeckenius (1981); Ropelewski and Halpert (1987); Lau and Sheu (1988); Kiladis and Diaz (1989). The rainfall data used here are the merged precipitation dataset for 1979–1992, prepared by Schemm *et al* (1992), which has been generated by combining observed monthly total precipitation data from the world surface station climatology (Spangler and Jenne (1990)) from NCAR and estimated oceanic precipitation from MSU measurements (Spencer (1993)). The observed spatial distribution of JJAS climatological (CLIM) rainfall rate is shown in figure 1.1. The most striking feature is the summer monsoon rainfall over India which has two maxima located over (**a**) northeast India and head Bay of Bengal and (**b**) west coast of India. Rainfall maxima in other regions of the tropics can be seen over equatorial western Pacific, highlands of Mexico, central America and equatorial South America and Africa. One can notice that the ITCZ lies to the north of equator almost encircling the entire globe. The composited global rainfall anomalies for the weak monsoon (WEAK-ISM) years is shown in figure 1.2. The principal regions associated with negative rainfall anomalies are the Indian summer monsoon region, equatorial western Pacific Ocean, Mexico and central America. One can notice an anomalous increase in rainfall over the equatorial central Pacific Ocean close to the dateline forced by the warm Pacific SST anomalies. The ENSO related rainfall anomaly in the equatorial Pacific Ocean extends from the central to eastern Pacific Ocean.

2.2 *Upper tropospheric circulations*

The 200 hPa circulations, based on the NCEP reanalysis data, for the CLIM case are shown in figure 2.1. The major climatological features to be noted are the upper tropospheric anticyclones over Tibet; the United States and Mexico. It can be seen that the subtropical westerlies are pushed sufficiently north of the Tibetan anticyclone. The TEJ associated with the summer monsoon can also be clearly observed. In addition, one can notice prominent upper

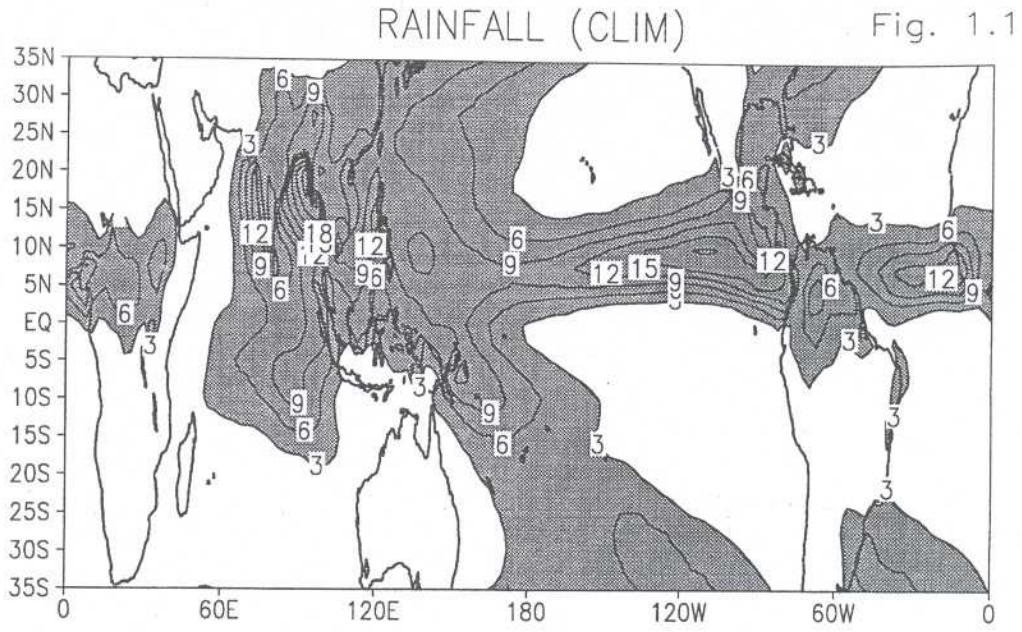

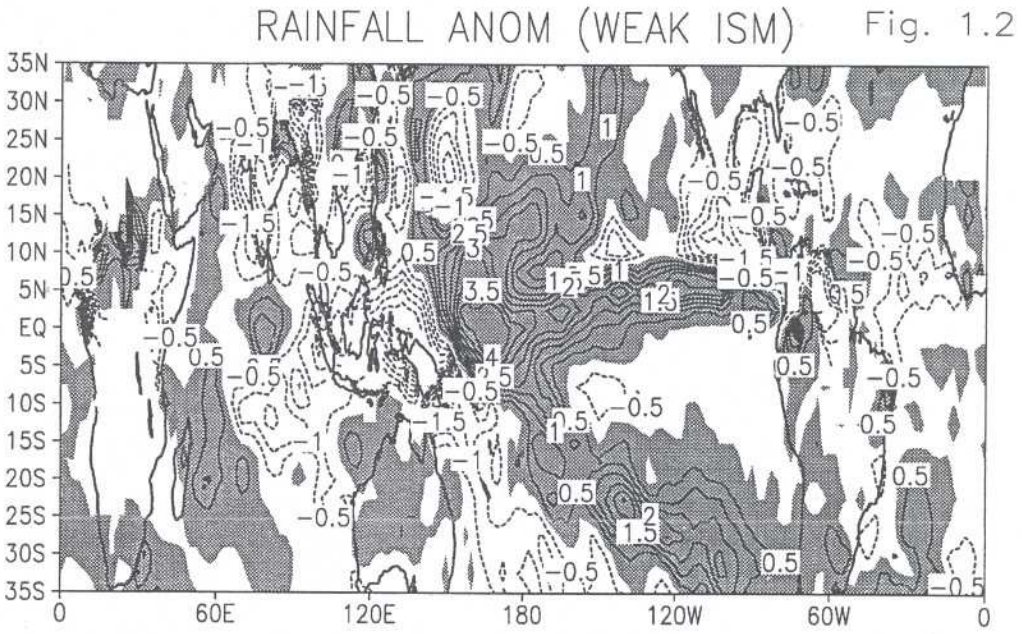

Figure 1.1. Observed JJAS mean climatological precipitation rate (mm day^{-1}). Contour interval is 3 units.
Figure 1.2. Composite of observed global rainfall anomalies (mm day^{-1}) for weak monsoon years. Contour interval is 0.5 units, zero contour is suppressed and negative values are shaded.

level trough patterns in mid-oceanic regions over the Pacific and Atlantic basins. It was Krishnamurti (1971a, b) who for the first time recognized that the tropical upper tropospheric circulations during the northern hemispheric summer were characterized by very large scale quasi-stationary cyclonic and anticyclonic circulations which were expressed mostly by the zonal wave numbers 1 and 2 and had a baroclinic structure in the vertical. Their study showed that these ultralong waves were maintained by land-ocean thermal contrast. The barotropic energetics calculation by Krishnamurti (1971a) and Kanamitsu *et al* (1972) revealed that the ultralong waves act as a kinetic energy source for smaller scales of motion and also for the zonal motion. The detailed diagnostic study of White (1982) showed that the summertime stationary eddies include two regimes: *tropical* and *high latitude*. The former is *global scale* and *monsoonal (baroclinic vertical structure)* and the latter is *smaller scale* and largely *barotropic*.

The upper level wind anomalies for the WEAK-ISM case are shown in figure 2.2. In this case, one can see anomalous cyclonic circulations over north-west India, Pakistan and also over the west coast of North America. The anomalous westerlies over India are indicative of a weakening of the TEJ. Over the tropical Pacific Ocean, one can see anomalous anticyclones straddling either side of the equator. There are

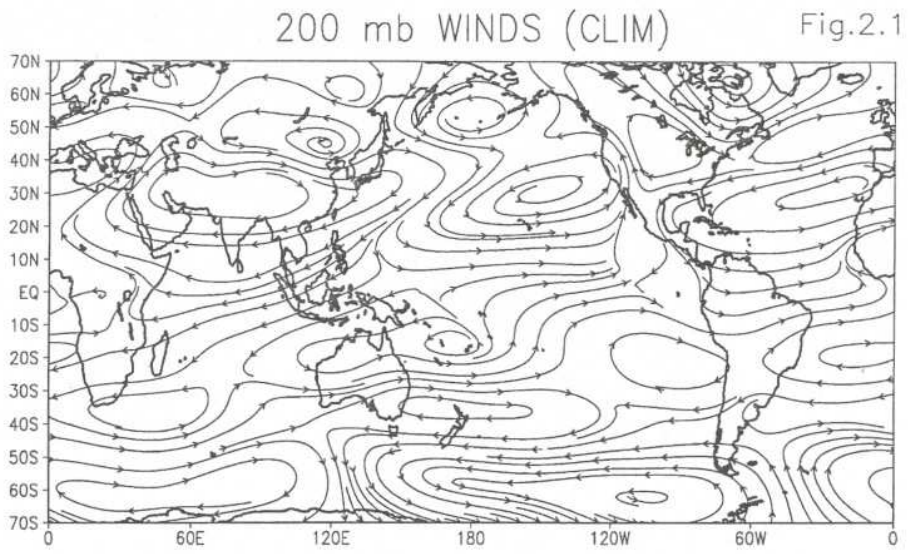

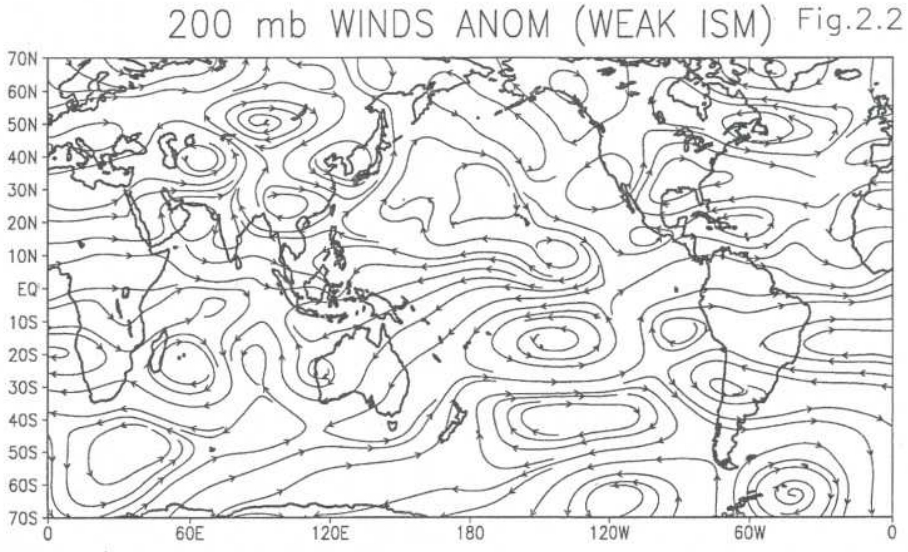

Figure 2.1. JJAS mean climatological zonally asymmetric (zonal mean removed) streamlines at 200 hPa from NCEP reanalysis.
Figure 2.2. Composite of 200 hPa zonally asymmetric streamline anomalies for weak monsoon years based on NCEP reanalysis.

anomalous upper level cyclones over southern Africa, south Indian Ocean and western Australia.

2.3 *Temperature field*

The 500 hPa climatological temperature field for the northern summer is shown in figure 3.1. One can see that the warmest region on the globe is located over the Tibetan plateau during the northern summer. This warming is largely associated with the release of latent heat over the elevated Tibetan plateau. It can be seen from figure 3.1, that the land regions over India and Tibet are significantly warmer than the tropical Indian and Pacific Oceans. These major land-ocean thermal contrasts (both in the north-south and east-west directions) essentially drive the summer monsoon circulations.

The 500 hPa temperature anomalies for the WEAK-ISM are shown in figure 3.2. The striking features are the warm thermal anomalies over the tropical central and eastern Pacific Ocean and cold thermal anomalies over west Asia, Iran, Pakistan, north of India, southern Russia and east Asia. The warm temperature anomaly seen over tropical central Pacific Ocean is largely related to latent heat release caused by moist convection due to the warm SST anomaly. Keshavamurty and Awade (1974) examined the upper air charts, prepared by the Institute of Meteorology, Free University of Berlin, and noted that the severe drought of 1972 over India was characterized by below normal tropospheric temperatures over southern parts of USSR (former Russia), Iran, Afghanistan, Pakistan and north India. These negative temperature anomalies are indicative of a

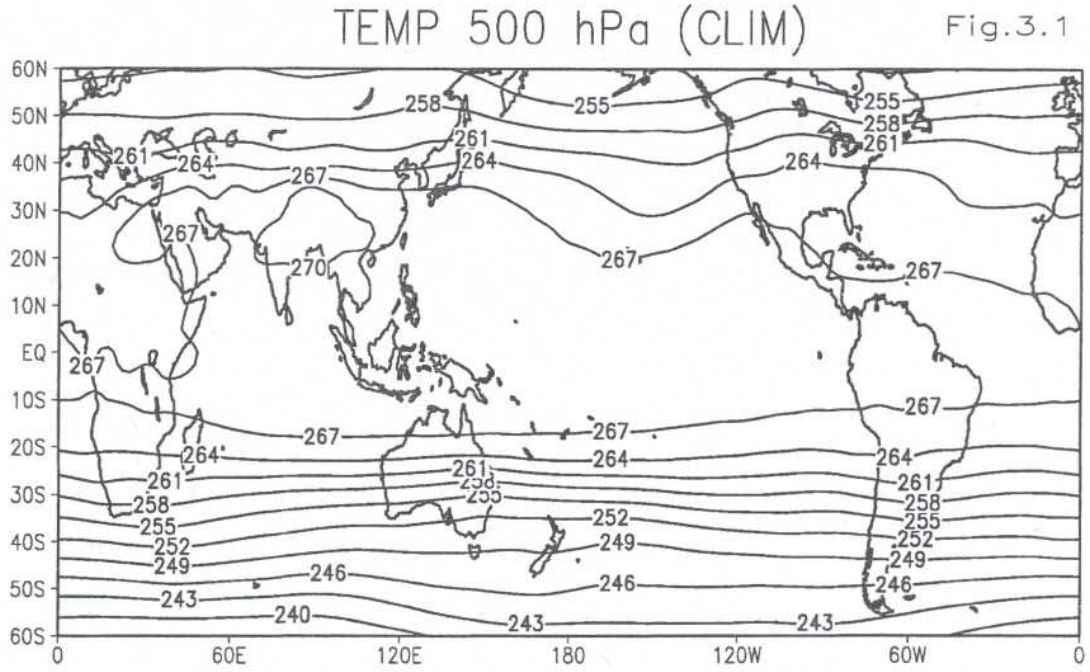

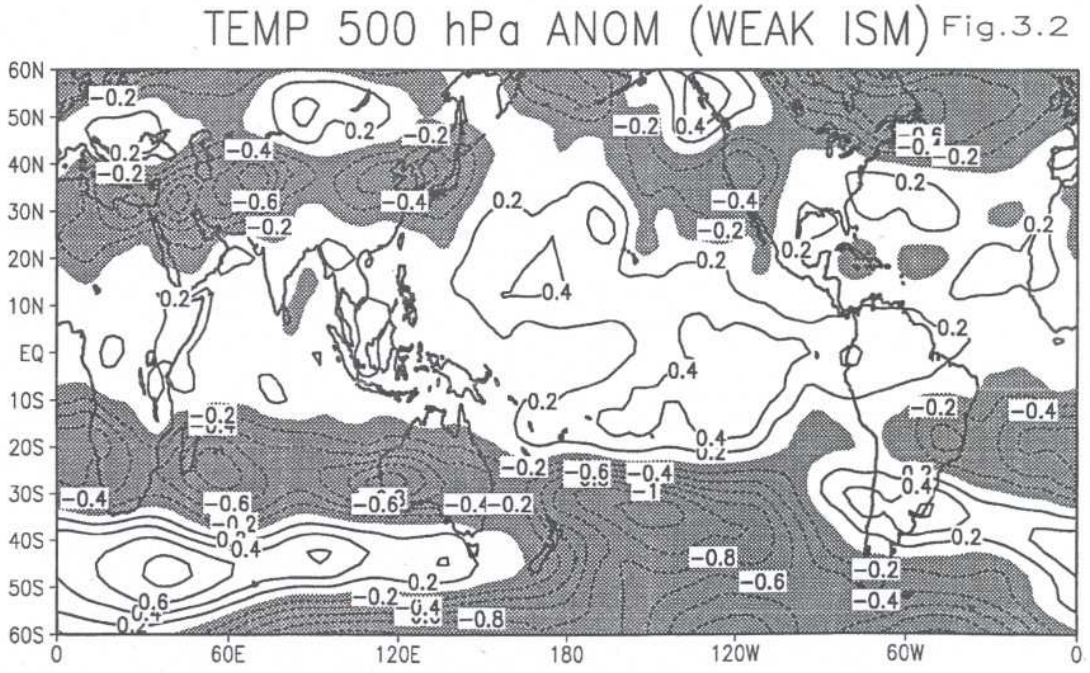

Figure 3.1. JJAS mean climatological temperature at 500 hPa from NCEP reanalysis, with contour interval of 3 K.
Figure 3.2. Weak monsoon composite of 500 hPa temperature anomalies based on NCEP reanalysis. Contour interval is 0.2 units, zero contour is suppressed and negative values are shaded.

reduction in the thermal forcing largely caused by a deep southward incursion of cold air from the mid-latitudes.

2.4 *Tropical pacific SST*

There is good observational evidence that a majority of bad monsoon years is associated with El Niño events in the equatorial Pacific Ocean (Sikka (1980); Pant and Parthasarathy (1981); Rasmusson and Carpenter (1983); Rasmusson and Wallace (1983); Ropelewski and Halpert (1987)). The SST data used here is from NCEP reanalysis which is based on Reynolds OISST – (Optimum Interpolated SST) (see Reynolds and Smith (1994)). Figure 4.1 shows the JJAS climatological SST over the tropical Pacific

Fig.4.1

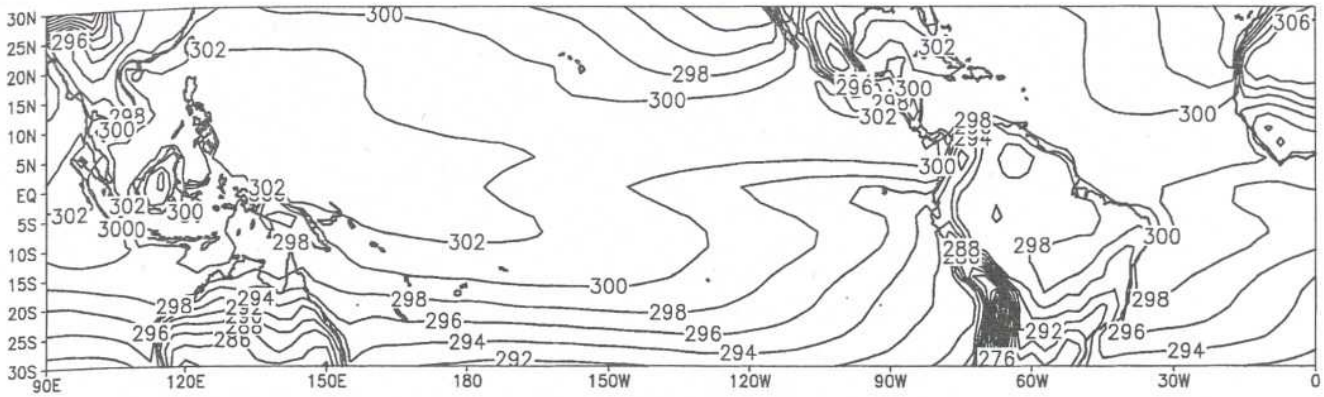

Fig.4.2

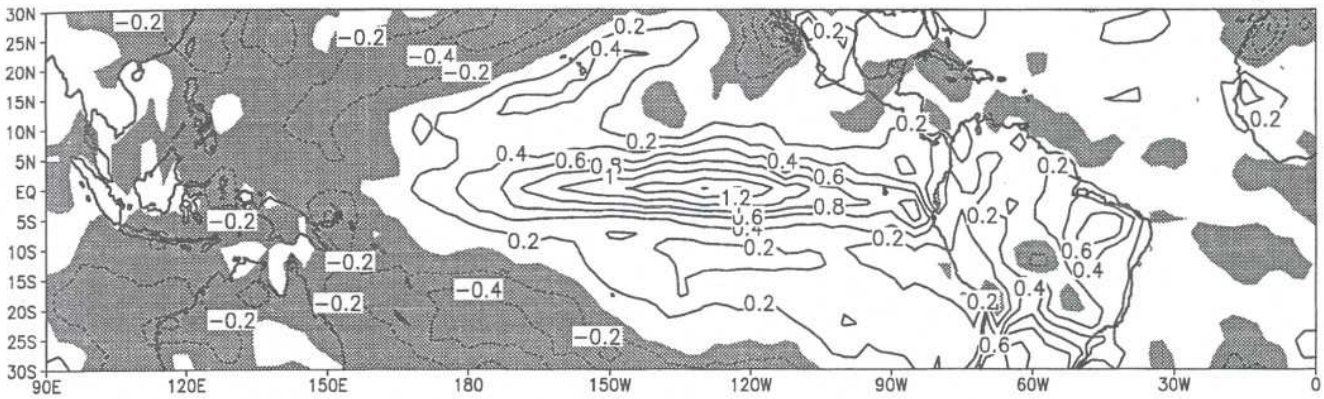

Figure 4.1. JJAS mean climatological surface temperature over the tropical Pacific Ocean from NCEP reanalysis. Contour interval is 2 K.

Figure 4.2. Composite of surface temperature anomalies for weak monsoon years over the tropical Pacific Ocean based on NCEP reanalysis. Contour interval is 0.2 units.

Ocean and figure 4.2 shows the corresponding SST anomalies for the WEAK-ISM case. It can be seen that the JJAS climatological SST over the equatorial western Pacific Ocean is relatively warmer than that of the eastern Pacific Ocean. However the WEAK-ISM anomalies in figure 4.2 show large positive SST anomalies in the central and eastern Pacific Ocean. Although the maximum amplitude of the Pacific SST anomalies in the composites is around 1.2°C, the ENSO related SST anomalies during individual years can be as large as 2–3°C.

2.5 *Upper tropospheric divergent circulations*

The velocity potential field (χ) associated with the divergent circulation has proven to be a very useful measure to identify the planetary scale monsoon. It was Krishnamurti (1971a) who for the first time illustrated the global structure of the summer monsoon by describing the planetary scale component of the monsoonal divergent circulations in terms of the χ-field. His study of the 200 hPa circulation patterns for summer 1967 revealed the existence of prominent east-west overturnings that were caused primarily because of the zonally asymmetric distribution of diabatic heating associated with the land-ocean thermal contrasts. The ascending branch of these monsoonal east-west cells, located at around 20°N, were quite different from the traditional equatorial Walker circulation. His study demonstrated that the upper tropospheric χ-field could be used to estimate the intensities of the monsoonal east-west and Hadley circulations during the northern summer. He noted that the intensity of the east-west circulation, in the Indian summer monsoon region, was comparable to that of the Hadley circulation. His study emphasized that the monsoonal divergent circulations played a crucial role in the generation of kinetic energy of quasi-stationary planetary scale waves.

The JJAS climatological divergent motions at 200 hPa computed from the NCEP reanalysis data are shown in figure 5.1. One can clearly recognize the dominance of wavenumber 1 structure in figure 5.1. The negative χ field over the monsoon region and Mexico represent the two main centres of divergent outflow in the upper troposphere. The descending branches of these divergent circulations lie over areas having positive χ field viz., equatorial central and eastern Pacific Ocean; the south Indian Ocean; Arabia and west Asia. From the divergent wind vectors one

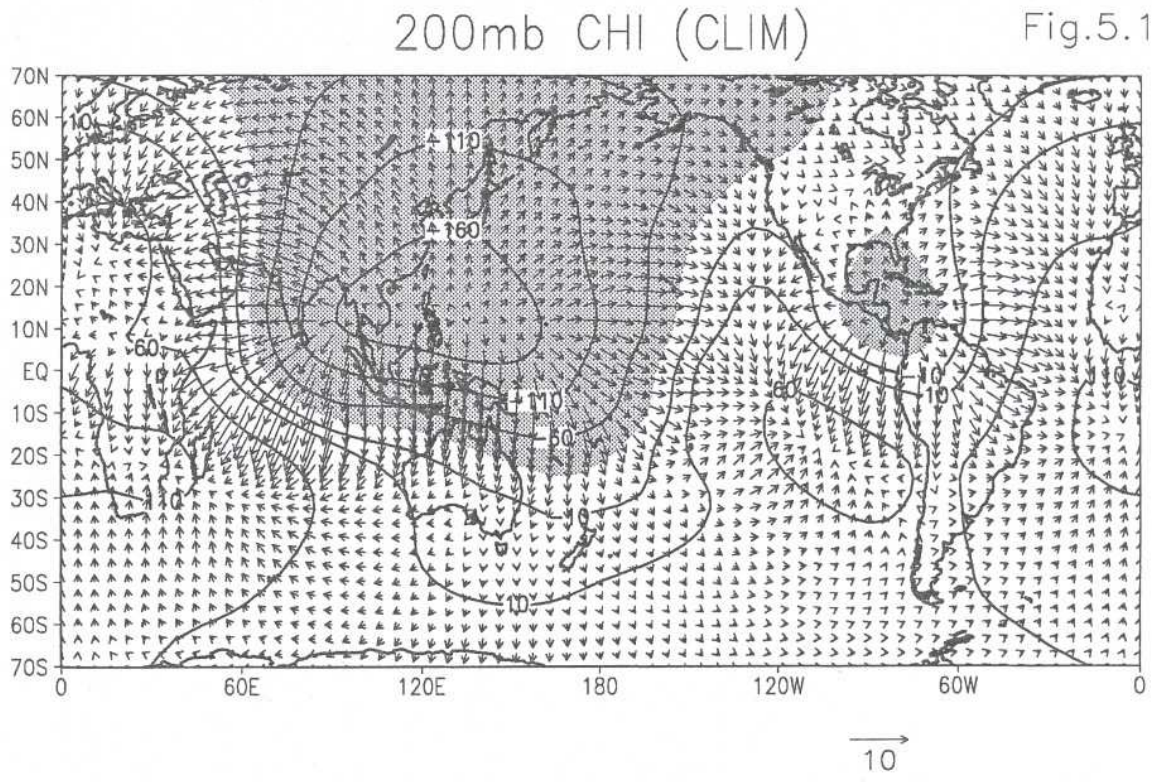

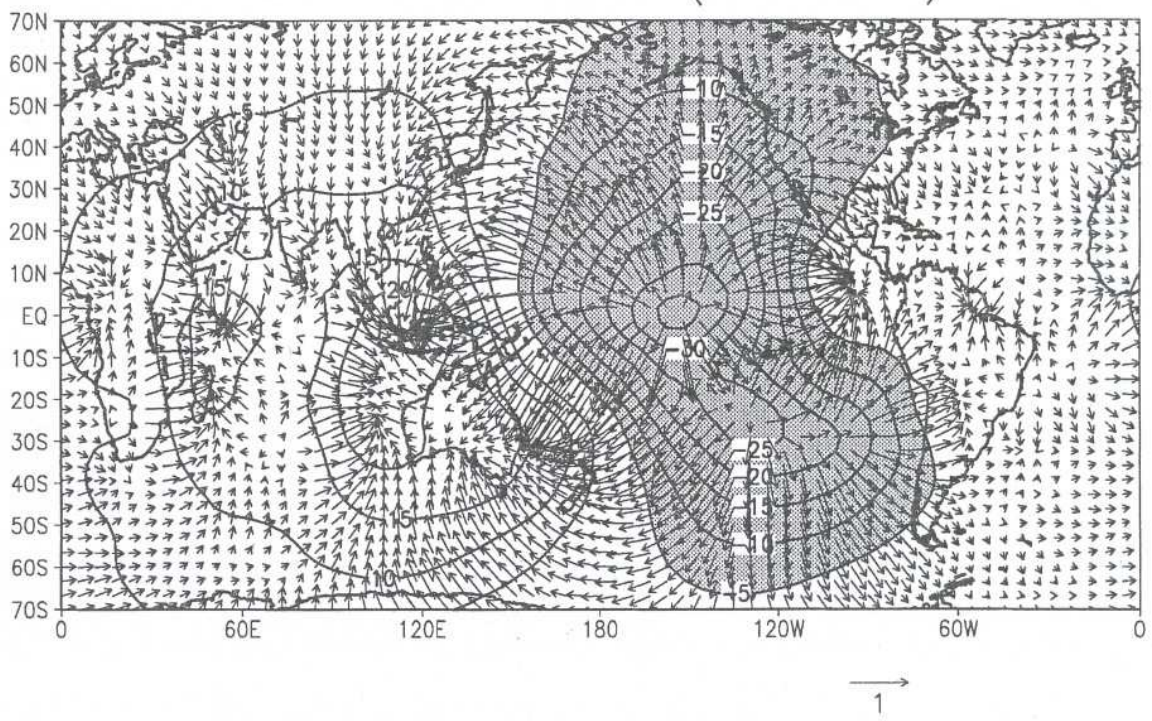

Figure 5.1. Climatological mean velocity potential ($X\,10^5 m^2\,s^{-1}$) at 200 hPa and divergent wind vectors. Contour interval is 50 units, negative contours are shaded and zero contour is suppressed.
Figure 5.2. Composite of 200 hPa velocity potential anomalies ($X\,10^5\,m^2\,s^{-1}$) for weak monsoon years from NCEP reanalysis. Contour interval is 5 units, negative contours are shaded and zero contour is suppressed.

can identify the equatorial Walker circulation, the monsoonal east-west circulations and the monsoonal north-south Hadley circulation.

The 200 hPa χ-anomalies for the WEAK-ISM are shown in figure 5.2. It can be seen that the anomalous divergent outflow in the upper troposphere has shifted

to the equatorial central and eastern Pacific sector. It is evident from the studies of Kanamitsu and Krishnamurti (1978); and Palmer *et al* (1992) that this displacement of divergent circulation anomalies is associated with the enhancement of local convective activity in the equatorial central-eastern Pacific Ocean because of the anomalous low level moisture convergence induced by the warm SST anomalies. One can notice from figure 5.2 that the anomalous descending motions occur over the equatorial western Pacific Ocean and the summer monsoon region. We have also examined the anomalous lower tropospheric divergent circulations for the WEAK-ISM case (figures not shown) and it is found that the monsoonal divergent circulations exhibit nearly out-of-phase patterns in the lower and upper troposphere indicating a baroclinic structure in the vertical.

3. Objectives of the present study

Earlier observational studies have noted that indications of the stationary wave anomalies associated with drought monsoon years can be traced back to the spring and previous winter months. Several other observational studies (Ramaswamy (1962); Ramamurthy (1969); and Raman and Rao (1981)) point out that breaks in the Indian summer monsoon are characterized by mid-latitude circulation anomalies similar to those seen during drought events. The fact that these quasi-stationary anomalies tend to persist over a long period of time makes them highly valuable from the point of long range forecasting of the Indian summer monsoon. This naturally arouses considerable scientific interest in learning more about the possible dynamical linkage between the stationary wave anomalies over India and the remote ENSO forcing over the tropical Pacific Ocean. Despite several observational and diagnostic studies in the past, very few modelling attempts have so far critically examined the dynamical mechanisms underlying the generation and maintenance of the summertime teleconnections over the Indian monsoon region. One of the primary objectives of this study is to understand the dynamical connection between ENSO and the summertime quasi-stationary anomalies over north India and neighbourhood. For this purpose we have carried out ensemble seasonal integrations with the COLA T30L18 atmospheric GCM. Details about the GCM and the ensemble integrations will be described in the forthcoming sections.

Another important question is the role of topography in modulating the summertime teleconnection anomalies induced by El Niño over the Indian monsoon region. The crucial role played by the topography of the Indian subcontinent in determining the summer monsoon rainfall was pointed out by Simpson (1921) in the early part of this century. His study suggested that a large percentage of rainfall over northern India, particularly the Gangetic plain, was induced because of orographic convergence due to the mountain ranges over the Indian subcontinent. Several studies based on simple models (Banerjee 1929; Sarkar 1966; Godbole 1973; Gadgil 1977) indicate that the orographic effect on the Indian summer monsoon activity is quite substantial. The influence of orography, particularly that of Himalayas, in maintaining the climatological features during the Northern summer monsoon has been amply demonstrated by quite a few GCM studies (Hahn and Manabe (1975); Gilchrist (1977); Broccoli and Manabe (1992); Ting (1994); and others). The results of Godbole (1973) and Hahn and Manabe (1975) suggest that in the absence of Himalayas, there is considerable weakening of the north-south pressure gradients over India and the Arabian Sea. In this paper, we shall address the question about the influence of Himalayas on the summertime anomalies seen over northwest India and neighbourhood during years of weak monsoon. More specifically, we wish to focus our attention on understanding the role of Himalayan orography in modulating the El Niño induced quasi-stationary anomalies over the Indian monsoon region. In order to study this problem, we have carried out several ensemble GCM experiments with and without mountains which will be described shortly.

4. Brief description of the GCM used

The model used in this study is the COLA (Center for Ocean-Land-Atmospheric Interactions) GCM, which evolved from the NMC spectral model described by Sela (1982). It is a global spectral model with triangular truncation at 30 waves and 18 levels in the vertical. A semi-implicit time integration scheme having a time-step of 15 minutes is used. Details about the parameterization of physical processes used in the model are given in table 1.

5. Details of model experiments

Keeping in mind the proposed objectives, we have carried out 3 cases (**C, E, NMA**) of 3-member ensemble seasonal integrations using the COLA GCM. The details of these GCM experiments are shown in table 2. The initial conditions are different for every member of an ensemble. Thus, for a given ensemble there are 3 GCM integrations which commence from 3 different initial conditions that are given in table 2. The idea behind carrying out ensemble seasonal runs is to determine the statistical significance of the results produced by the GCM simulations. All the seasonal integrations terminate on 1st

Table 1. *Description of GCM.*

COLA AGCM	Spectral (T30); 18 σ-levels.
Prognostic variables	ζ; D; T; q; $\ln(p_s)$.
Time integration	Semi-implicit (time step 15 min).
Horizontal diffusion etc.,	∇^4; Roberts time filter; Gravity Wave Drag.
Latent heating	Large scale condensation. Convective (Kuo (1965); Anthes (1977)). Shallow convection (Tiedke (1984)).
Radiation	Short wave (Lacis and Hansen (1974)) (CALL 1hr). Long wave (Harshvardhan *et al* (1987))(CALL 3hr).
PBL	Mellor-Yamada (1982).
Biosphere	Simple biosphere (SiB) (Xue *et al* (1991)).

Table 2. *Experimental design.*

Experiment	Ensemble runs	Initial condition	SST	Orography
C	C1	01 June 1986	CLIM SST	Yes.
	C2	01 June 1987	CLIM SST	Yes.
	C3	15 May 1988	CLIM SST	Yes.
E	E1	01 June 1986	ANOM SST	Yes.
	E2	01 June 1987	ANOM SST	Yes.
	E3	15 May 1988	ANOM SST	Yes.
NMA	NMA1	01 June 1986	ANOM SST	No.
	NMA2	01 June 1987	ANOM SST	No.
	NMA3	15 May 1988	ANOM SST	No.

October. The ensemble averages of the various fields are analyzed for all the three cases.

Experiment **C** uses monthly mean climatological Reynolds SST as lower boundary forcing (figure 6.1). In experiment **E**, an idealized symmetric SST anomaly (figure 6.2) in the equatorial eastern-central Pacific Ocean, similar to that used by Keshavamurty (1982), is superposed on the monthly mean climatological Reynolds SST. It must be mentioned that the location and amplitude of the idealized anomaly match well with the observed anomaly (see figure 4.2). As the spatial structure of the actual SST anomalies are quite complicated and differ from year to year, the use of an idealized equatorially symmetric SST anomaly can simplify the interpretation of model results and facilitate an easier understanding of the role of ENSO in generating teleconnection patterns over the Indian summer monsoon region. The summertime anomalous response induced by ENSO can be understood by comparing the simulations in **C** and **E**.

Experiment **NMA** uses an idealized symmetric SST anomaly superposed on the monthly mean climatological Reynolds SST, but the mountains (e.g., Himalayas, Rockies, Andes etc.,) are excluded from the GCM in this case. It is important to mention here that the COLA GCM used in the present study, employs mean orography. The study by Fennessy *et al* (1994) suggests that the use of mean orography in the COLA GCM results in more realistic simulations of the Indian summer monsoon circulation and rainfall as compared to simulations based on silhouette orography. We would like to further add that in the **NMA** experiment, the GCM initial conditions (i.e., mass and wind fields) have been consistently adjusted so as to account for the removal of topography. A comparison of experiments **C** and **NMA** is supposed to bring out the combined effects of ENSO and orographic forcings on the anomalous summertime response.

6. Results and discussions

6.1 *Rainfall simulations*

The ensemble average of the simulated precipitation for **C** (figure 7.1) shows rainfall over the summer monsoon region, western Pacific and along the ITCZ over equatorial South America and Africa. Although there are discrepancies in realistically capturing the regional precipitation patterns over India, like the maxima over west coast and the head Bay of Bengal, one can notice that the GCM is able to carry the summer monsoon rainfall northward beyond 20°N.

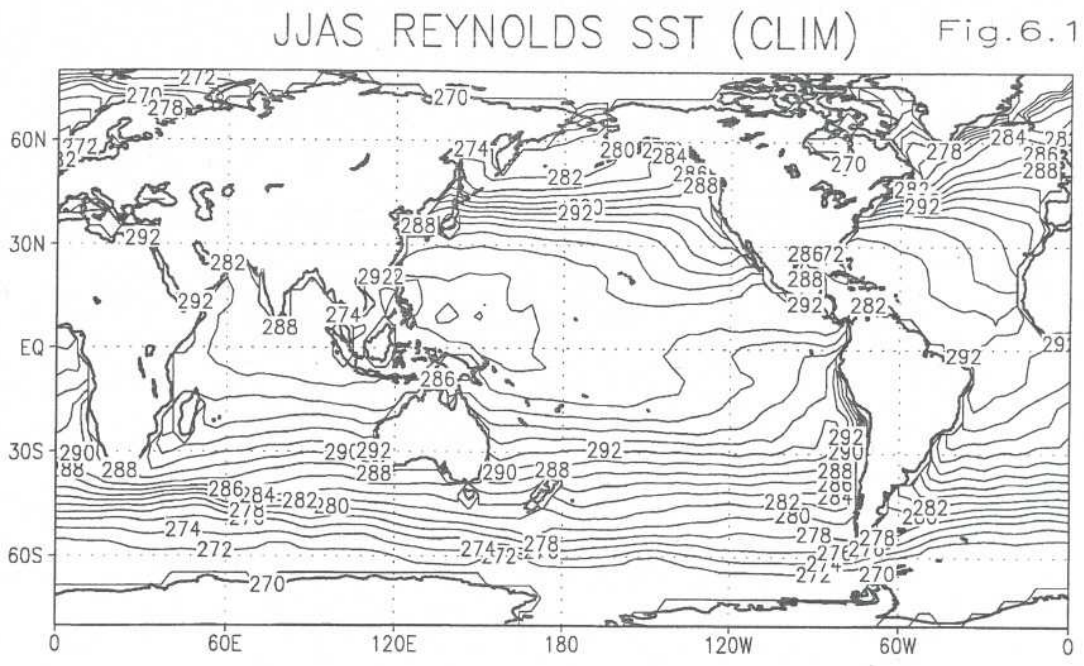

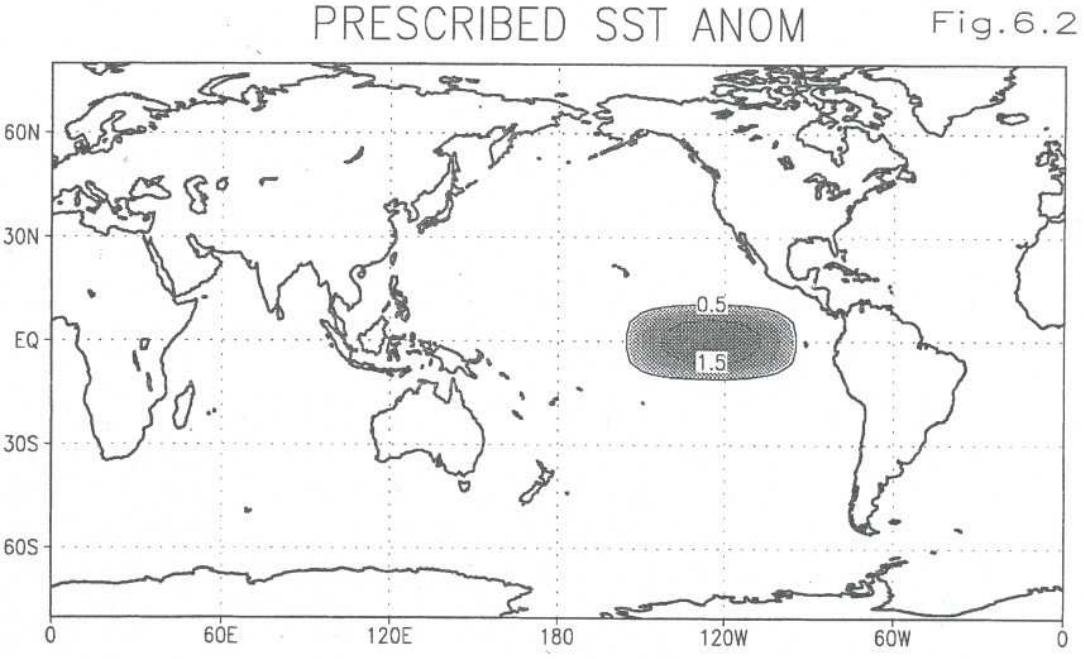

Figure 6.1. JJAS mean climatological global SST. Contour interval is 2 K.
Figure 6.2. Idealized symmetric SST anomaly over the equatorial eastern-central Pacific Ocean used in this study. Contour interval 1 K.

Considering the coarse resolution of the GCM and also the fact that most of the state-of-the-art climate GCMs are not able to simulate Indian monsoon rainfall adequately well, one must mention that the present simulation is quite reasonable in producing sufficient northward shift of the rainfall pattern over the summer monsoon region. It may be mentioned that the primary purpose of the present work is to understand the dynamics of the ENSO induced teleconnections over the Indian monsoon region rather than to focus critically on the accuracy of the monsoon rainfall simulations.

The difference (**E-C**) of the rainfall simulations (figure 7.2) shows the precipitation anomalies in response to the warm SST anomaly in the equatorial eastern-central Pacific Ocean. One can clearly see that there is an increase in rainfall over the region of warm SST forcing and a simultaneous decrease over the western Pacific Ocean. This anomalous rainfall distribution over the Pacific Ocean is typical of warm

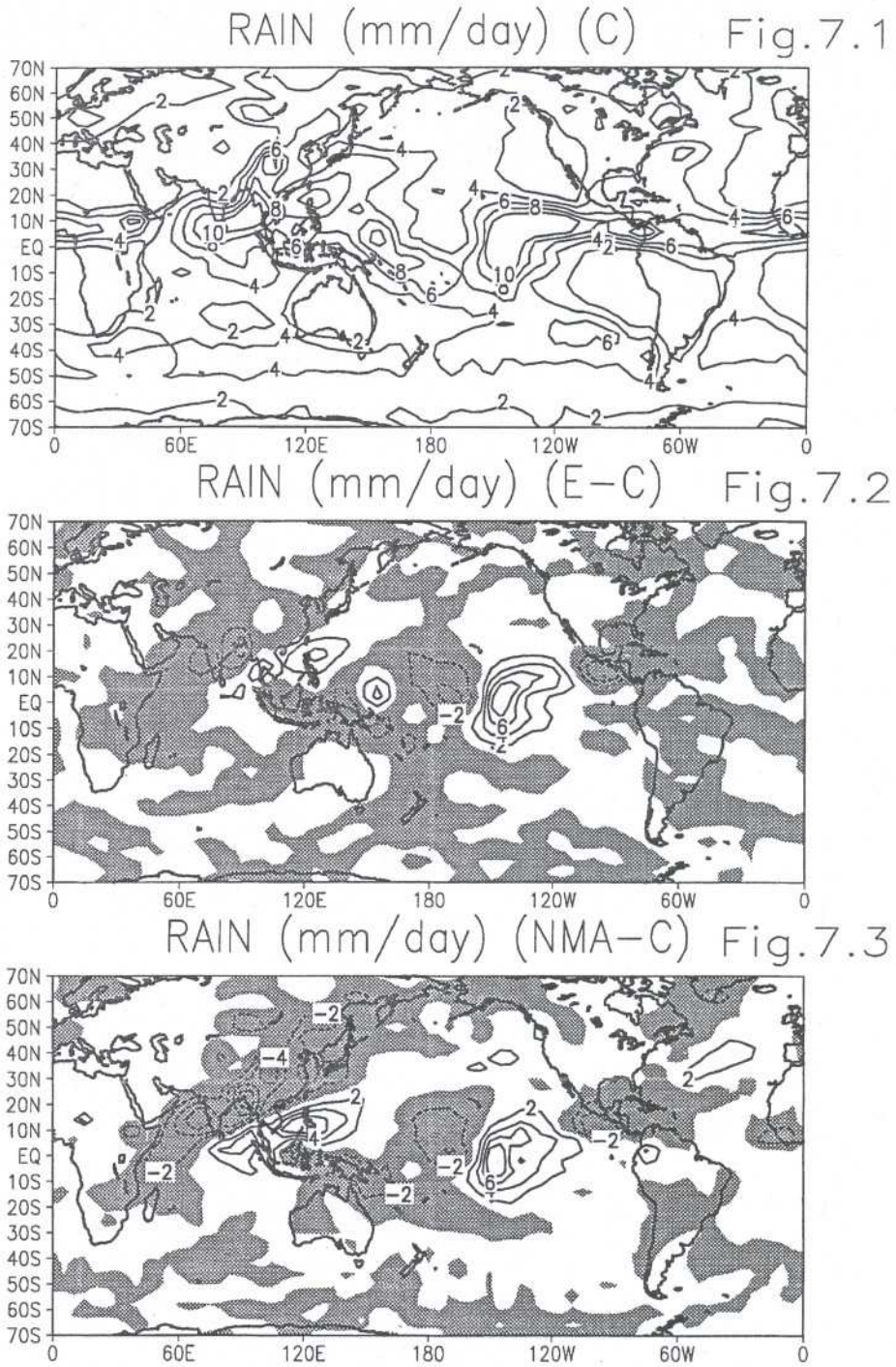

Figure 7.1. Simulated JJAS mean precipitation rate (mm day^{-1}) for **C**. Contour interval is 2 units.
Figure 7.2. Same as figure 7.1 except for **E-C**.
Figure 7.3. Same as figure 7.1 except for **NMA-C**.

ENSO events. Also there is a decrease in rainfall over central America and Mexico. It is more important to note that there is a substantial decrease in the monsoon rainfall over India. At a later stage we shall show that the Indian monsoon rainfall anomaly induced by ENSO is indeed statistically significant. These results are consistent with the past observational findings (see section 1.1) and also agree well with the modelling studies of (Keshavamurty (1982); Palmer *et al* (1992); Brankovic *et al* (1993); Shukla and Fennessy (1994); Sperber *et al* (1994); Krishnan and Fennessy (1997)). The positive rainfall anomaly over south China sea seen in figure 7.2 could be due to the ENSO induced eastward shift of the monsoonal divergent circulations, as it occurred during the summer of 1987 (see Krishnamurti *et al*

(1989)) which resulted in excess rainfall over parts of China.

The combined effects of the neglect of orography and the influence of ENSO forcing on the summer monsoon rainfall are illustrated by the difference (**NMA-C**) in figure 7.3. One can notice a very large decrease in the summer monsoon rainfall over India and east Asia. A comparison of figures 7.2 and 7.3 suggests that this large decrease in rainfall over India and east Asia is mainly attributable to the removal of orography in **NMA**. This is consistent with the model simulations of Godbole (1973) and Hahn and Manabe (1975) which demonstrated that neglecting the Himalayas would produce a major weakening of convective heating over the elevated Tibetan Plateau and consequently lead to a subdued rainfall activity over India. The excess precipitation over equatorial Indian and western Pacific Oceans seen in figure 7.3 suggests that the neglect of Himalayas in **NMA** does not favour the northward advance of the monsoon rainfall into the subcontinent. The decrease of rainfall over the land region and the increase of rainfall over the equatorial oceans in the **NMA** experiment is suggestive of a major reduction in the north-south differential heating over the monsoon region. By comparing figures 7.2 and 7.3 one can infer that the removal of orography in the **NMA** experiment does not lead to substantial changes over the tropical central-eastern Pacific Ocean. The precipitation anomalies in figure 7.3 over the central-eastern Pacific Ocean can be mostly ascribed to the local impact of the warm SST forcing. We shall at a later stage show that these anomalous precipitation patterns are statistically significant.

6.2 *Simulated upper tropospheric divergent circulations*

The 200 hPa χ-field for **C** is shown in figure 8.1. The negative (positive) areas correspond to regions of divergent outflow (inflow) in the upper troposphere. The divergent winds blow in a direction normal to the contours of χ. Closely (widely) spaced contours indicate that the strength of the divergent winds is strong (weak) respectively. From figure 8.1 one can see a divergent outflow over the Indian and Asian summer monsoon regions; a sinking motion over the eastern end of the Pacific Ocean and a strong subsidence over Iran and Arabia towards the west. These correspond to the east-west monsoonal circulations identified by Krishnamurti (1971b). He estimated the intensities of the east-west circulations and Hadley type circulation from the zonal and meridional gradients of the (χ) field. Krishnamurti *et al* (1990) further noted that strong monsoons, like that of 1988, are characterized by highly intense and spatially gigantic east-west circulations. It can be noted that the GCM simulated divergent outflow over the monsoon region is relatively underestimated as compared to observations. In the north-south direction, the descending branch of the divergent motions is seen over the south Indian Ocean. This corresponds to the monsoon Reverse Hadley circulation.

The difference (**E-C**) in the simulated velocity potential in figure 8.2 shows that the SST forcing in **E**, shifts the centre of action to the equatorial eastern Pacific Ocean. The negative anomalies over the eastern Pacific Ocean suggest that there is an enhanced upper level divergent outflow over this area; the positive anomalies over the summer monsoon region and western Pacific Ocean indicate that there is an anomalous sinking over this region. The GCM simulated divergent circulation anomalies over the monsoon region and the tropical Pacific Ocean are much stronger than the observed anomalies. Major eastward shifts of the monsoonal east-west circulations during El Niño years were observed by Kanamitsu and Krishnamurti (1978); Krishnamurti *et al* (1989); and subsequently seen in the GCM simulations of Palmer *et al* (1992). Krishnamurti and Surgi (1987) have pointed out that the effect of ENSO on the Indian summer monsoon is nearly simultaneous and occurs via., changes in the monsoonal divergent circulations. Though the simulated divergent circulation anomalies are somewhat stronger in amplitude, their spatial distribution matches reasonably well with the observed anomalies (figure 5.2).

The combined effects of the neglect of orography and the presence of ENSO forcing on the divergent circulations are illustrated by the difference (**NMA-C**) in figure 8.3. The large upper level convergence anomaly over India and Asia indicates a strong anomalous subsidence over the monsoon region. By comparing figures 8.2 and 8.3, it can be seen that the drastic weakening of the divergent circulations locally over the monsoon region in **NMA** has significant contributions both because of neglect of orography and also due to the Pacific SST forcing. The weakening of the divergent outflow in **NMA** over the monsoon region arising from the removal of the orography is related to a major decrease in moist convection over the Tibetan region. It is evident from figures 8.2 and 8.3 that the anomalous divergent outflow in **NMA** over the equatorial eastern Pacific Ocean is largely due to the warm SST anomaly.

6.3 *Simulated upper tropospheric flow patterns*

The simulated streamlines at 200 hPa level for experiment (**C**) are shown in figure 9.1 The important features to be noted in the simulation are the upper tropospheric anticyclones over Tibet, United States and the Mexican highlands. It can be seen that the subtropical westerlies over the monsoon region are pushed sufficiently northward into the extratropics. The TEJ associated with the summer monsoon is also

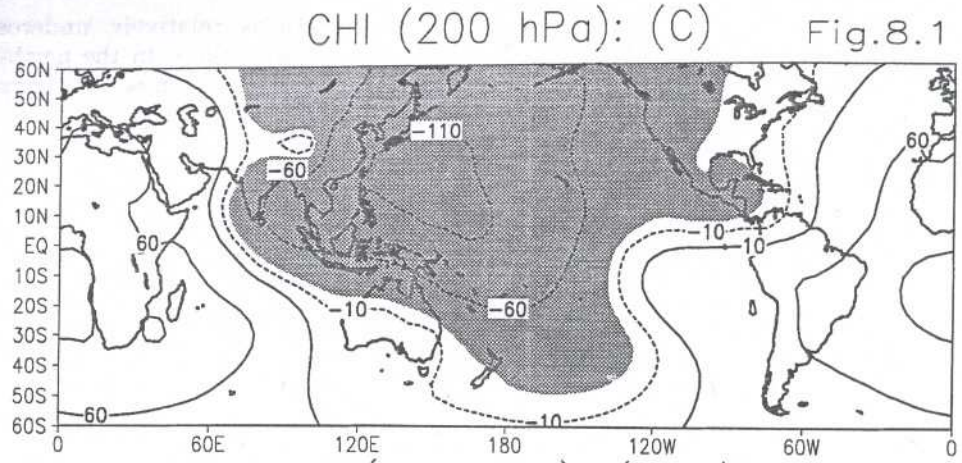

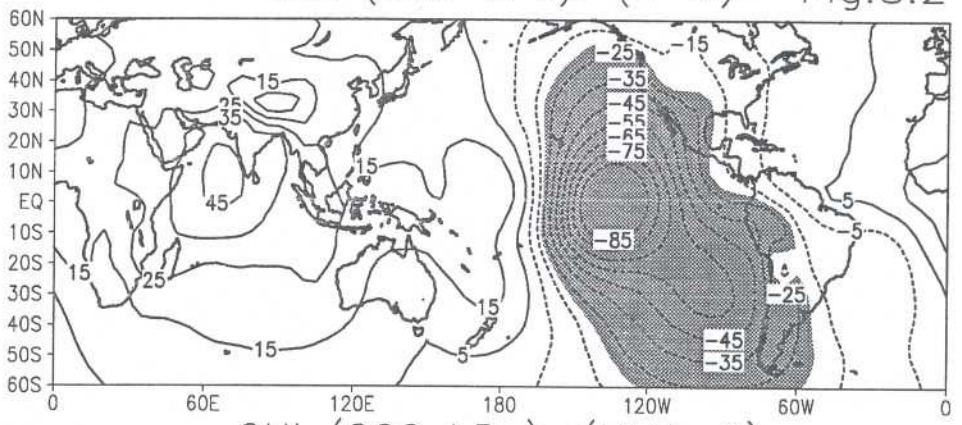

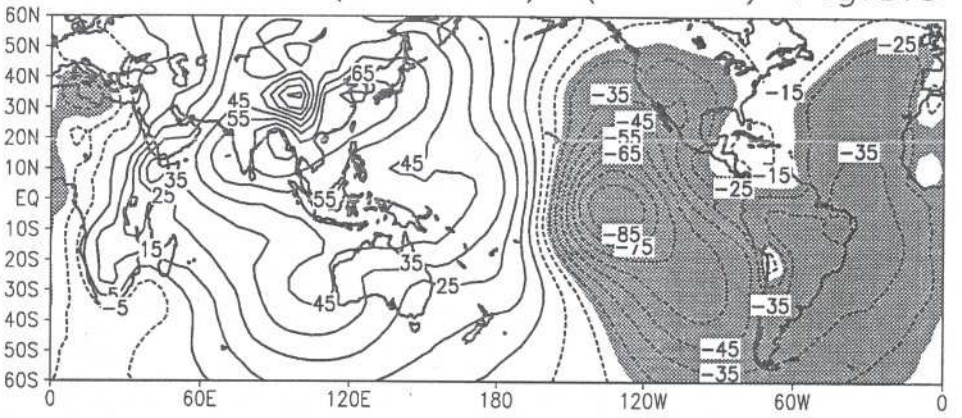

Figure 8.1. Simulated JJAS mean velocity potential (X 10^5 m^2 s^{-1}) at 200 hPa for **C**. Contour interval is 50 units, zero contour is suppressed and negative values are shaded.
Figure 8.2. Same as figure 8.1 except for **E-C**. Contour interval is 10 units.
Figure 8.3. Same as figure 8.1 except for **NMA-C**. Contour interval is 10 units.

captured well in the GCM simulation. The upper tropospheric mid-oceanic troughs in the Pacific and Atlantic Oceans can also be seen in the GCM simulations. Overall, the GCM is able to capture quite realistically most of the climatological features over the tropical areas, which is essential for any model that attempts to simulate the summer monsoon (Krishnamurti *et al* (1973)).

The difference (**E-C**) in the simulated 200 hPa streamlines are shown in figure 9.2. In the equatorial eastern Pacific Ocean, one can observe upper level easterly (westerly) anomalies on the western (eastern) side of the SST forcing, caused by a local enhancement of moist convection in **E**. The anomalous equatorial easterlies to the west of the heat source are suggestive of a weakening of the equatorial Walker circulation.

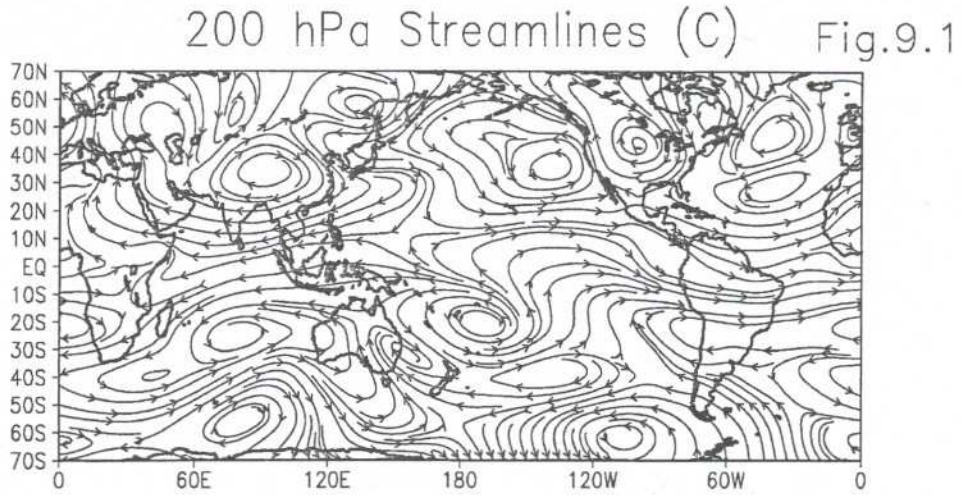

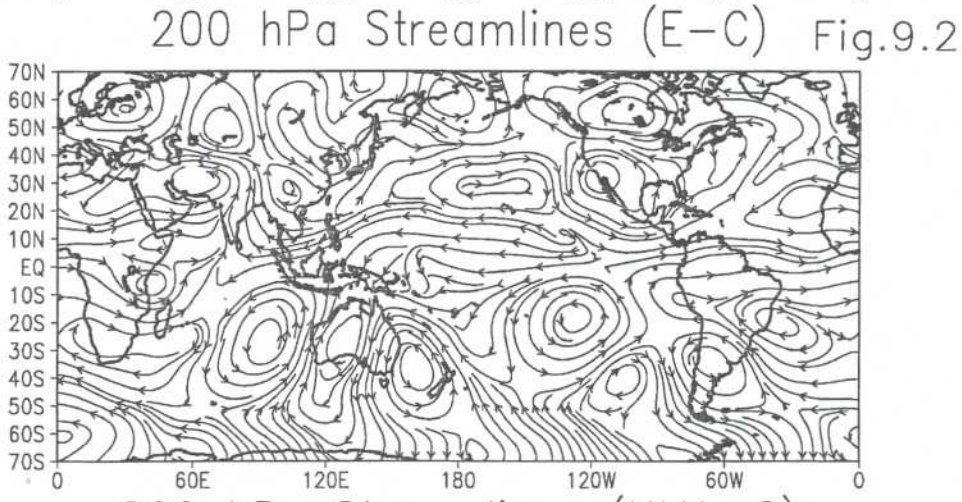

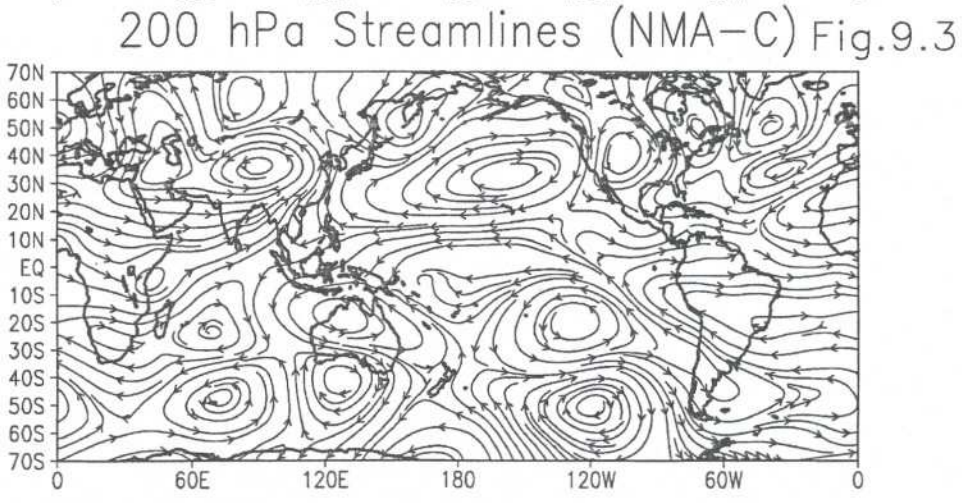

Figure 9.1. Simulated zonally asymmetric streamlines at 200 hPa for **C**.
Figure 9.2. Same as figure 9.1 except for **E-C**.
Figure 9.3. Same as figure 9.1 except for **NMA-C**.

To the west of the heat source, one can notice a pair of anomalous anticyclones flanking the equator in both the hemispheres, which is a characteristic feature seen during warm episodes. Based on the classical works of Matsuno (1966), and Gill (1980), one might roughly interpret the equatorial westerly response to the east of the heat source as Kelvin waves and the anomalous response to the west of the symmetric heat source as Rossby waves. The southern hemispheric anticyclone is stronger in intensity and well organized than the one in the northern hemisphere. It may be noted that the warm Pacific SST anomaly induces upper level

cyclonic circulation anomalies over North America and Mexico which indicate a weakening of the high over those regions which is consistent with observations. There are several other interesting extratropical features in figure 9.2. For instance one can notice an extratropical cyclone over Europe which is followed by an anticyclonic anomaly centered around 75°E, 55°N which in turn is followed by a cyclonic anomaly with center around 110°E, 50°N. It appears that the sequence of anomalous cyclones and anticyclones in the higher latitudes is a combined nonlinear effect produced by the Pacific SST forcing and the Himalayan topography. The series of alternating anticyclones and cyclones to the east of the Himalayas, both in the subtropics and extratropics, are suggestive of "Lee Waves" which occur due to impingement of westerlies on the western end of the mountain barrier. The dynamics of these lee waves can be explained by applying the conservation of potential vorticity for a westerly flow over a topographic barrier (see Holton (1979), pp 89–90).

In addition to the anomalies seen locally over the tropical Pacific basin, it is of considerable interest to take note of the remote response over the summer monsoon region. From figure 9.2, one can see anomalous westerlies extending all the way from northern Africa and Arabia into central and peninsular India. These anomalous features suggest a major weakening of the Tibetan anticyclone and the TEJ. An anomalous cyclonic circulation in the higher latitudes can be seen extending zonally from Europe, west Asia, Pakistan up to northwest India. These extratropical cyclonic anomalies tend to advect cold air from higher latitudes into the monsoon region. This incursion of cold westerlies into north India can reduce the north-south thermal contrast and in turn weaken the intensity of the monsoonal large scale circulations. Thus the Pacific SST forcing induces two major effects on the Indian summer monsoon (**1**) produces anomalous westerlies over the tropics which counteracts the monsoon TEJ (**2**) induces cyclonic anomalies over northwest India by modulation of the mid-latitude westerly flow. Both these effects oppose the summer monsoon activity over India. The model simulated anomalies in **E-C** match quite well with the observed features normally seen during drought years over the summer monsoon region.

We shall now examine the combined effects of warm Pacific SST anomalies and the neglect of orography on the summertime circulations. The difference (**NMA-C**) in the simulated streamlines (figure 9.3) shows very large circulation anomalies over the summer monsoon region. It can be seen that the neglect of topography in the GCM, results in a strong anomalous cyclonic circulation that covers north India and a large region of Asia. One can see anomalous westerlies extending over the entire monsoon region implying a large weakening of the summer monsoon. By comparing figures 9.2 and 9.3, it can be readily observed that the weakening of the regional monsoonal circulations resulting from neglect of orography is more pronounced than that resulting from the Pacific SST forcing. For instance, the extratropical cyclonic anomaly in figure 9.2 is confined to northern Europe and its subtropical counterpart extends up to northwest India. On the other hand the extratropical cyclonic anomalies in figure 9.3 have penetrated very much into the monsoon region because of the absence of the Himalayan barrier. In other words, the presence of Himalayas effectively anchors the extratropical troughs induced by El Niño in the higher latitudes in **E**, thereby playing a major role in restricting the southward incursion of mid-latitude waves and in turn mitigating the adverse consequences on the summer monsoon activity over India. It was earlier seen in figure 7.3 that the **NMA** experiment produces significant precipitation anomalies over the monsoon region. Associated with these precipitation changes one can expect significant heating anomalies over the monsoon region. It must be mentioned that these local heating anomalies in the **NMA** experiment can induce stationary wave anomalies in the wind field which add on to the changes in the orographically induced stationary waves. It is however beyond the scope of the present work to isolate these two different effects. It is interesting to note from figures 9.2 and 9.3, that the El Niño induced circulation anomalies over the tropical eastern Pacific Ocean are subjected to considerable orographic modification. It can be seen that the northern hemispheric anticyclonic anomaly over the tropical eastern Pacific Ocean is better organized in **NMA** as compared to **E**. Likewise one can notice substantial orographic influence on the anomalous circulations in the southern hemispheric extratropics.

6.4 *Simulated temperature fields*

The simulated 500 hPa temperature field in **C** is shown in figure 10.1. One can see that the warming over the monsoon region is reasonably captured by the GCM. The thermal contrast between the Asian land mass and the tropical Indian and Pacific Oceans is seen in the GCM simulation. Over the mid-oceanic troughs of north Pacific and north Atlantic, one can notice that the thermal field is slightly oriented from southwest to northeast. The GCM simulated mid-tropospheric temperatures over the monsoon region are slightly smaller when compared to those of the NCEP reanalysis (figure 3.1). Despite these minor discrepancies, there is an overall agreement between the simulated and observed thermal patterns.

The difference **E-C** of the 500 hPa temperature field is shown in figure 10.2. It is important to note the occurrence of negative temperature anomalies over west Asia, Afghanistan, Pakistan and northwest India.

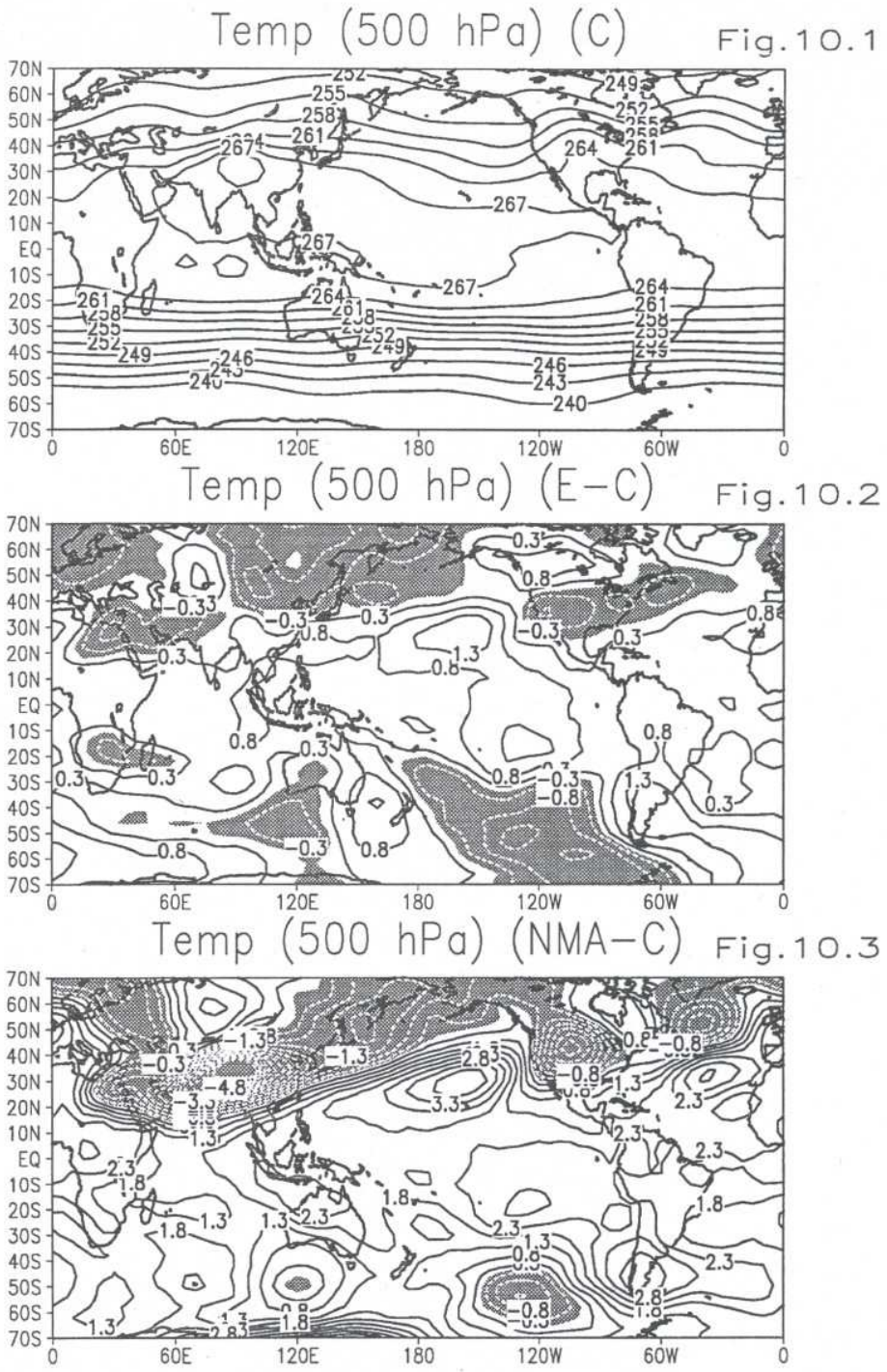

Figure 10.1. Simulated temperature field at 500 hPa for **C**. Contour interval is 3 units.
Figure 10.2. Same as figure 10.1 except for **E-C**. Contour interval is 0.5 units, zero contour is suppressed and negative values are shaded.
Figure 10.3. Same as figure 10.1 except for **NMA-C**. Contour interval is 0.5 units, zero contour is suppressed and negative values are shaded.

The simulated thermal anomaly over this region is slightly smaller in magnitude when compared to the observed anomalies (figure 3.2). One can also see negative thermal anomalies over northeast Asia and over large regions of North America which are reasonably consistent with observations. The anomalous warming of the mid-troposphere over the tropical eastern-central Pacific is also seen in the GCM simulations. However the simulated anomalies in the tropical Pacific are stronger in magnitude and displaced more northward as compared to the observed anomalies. Excluding these differences, the simulated and observed anomalies seem to agree grossly well.

The difference **NMA-C** of the 500 hPa temperature field is shown in figure 10.3. Large negative

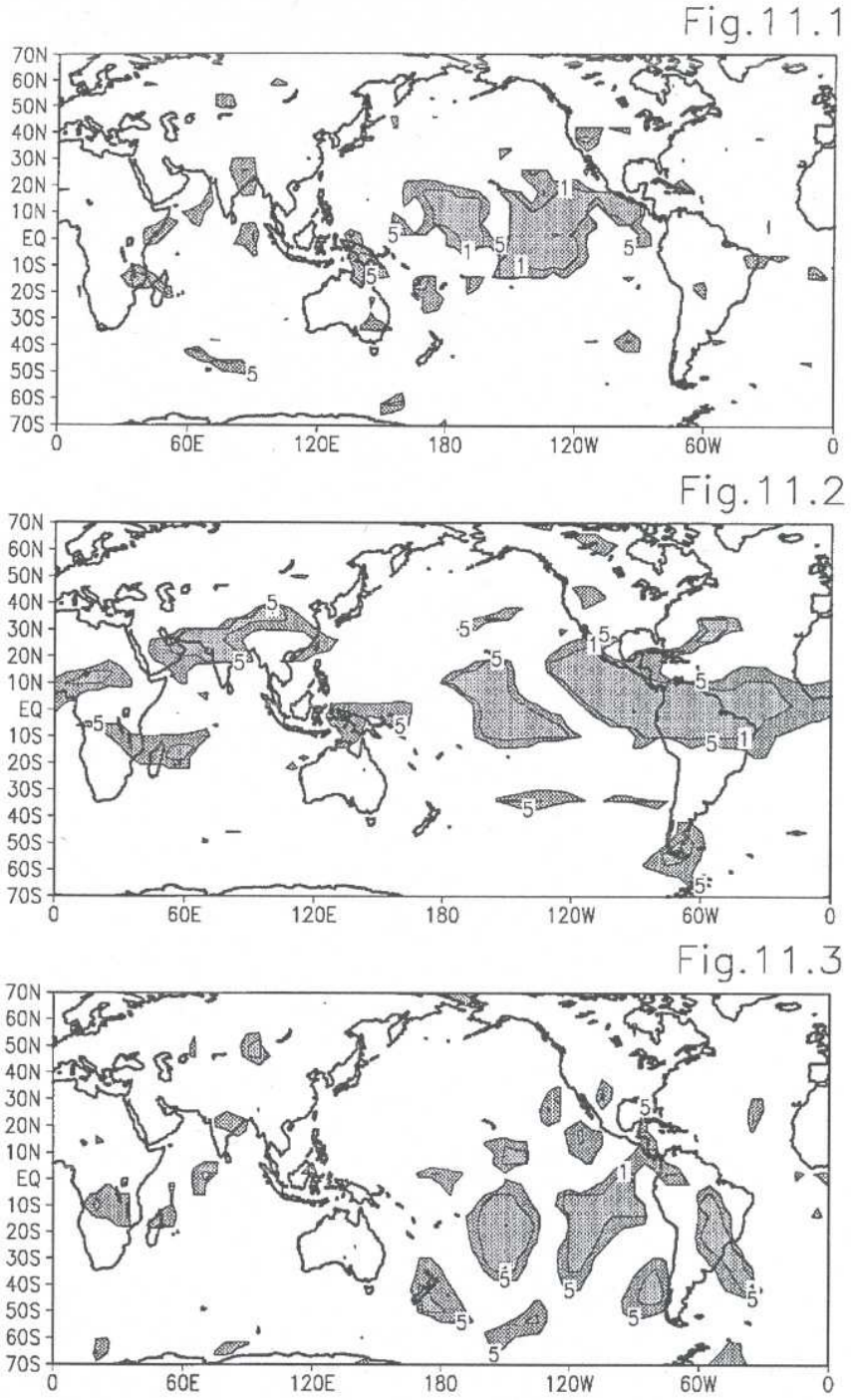

Figure 11. Statistical significance levels (%) from t-test for **C** and **E**. Levels above 5% significance are not shown; (11.1) Rainfall; (11.2) u – 200 hPa; (11.3) v – 200hPa.

thermal anomalies can be conspicuously seen extending zonally eastward from north Africa up to central Asia. It is evident from figures 10.2 and 10.3, that this anomalous feature is mainly associated with the neglect of Himalayan orography in **NMA**. In the absence of the Himalayas, there is a large decrease in moist convective heating over the Tibetan plateau in **NMA** which explains the widespread negative anomaly in figure 10.3. One can also notice considerable modification of the thermal anomalies in the Pacific Ocean. For instance, a large positive anomaly can be seen over the north Pacific Ocean. By comparing figures 10.2 and 10.3, it is clear that the orographically induced thermal changes are very prominent in the northern hemispheric extratropics.

7. Statistical significance test

From the results of the ensemble integrations, we have carried out statistical tests, using the classical t-test as in Chervin and Schneider (1976), in order to evaluate

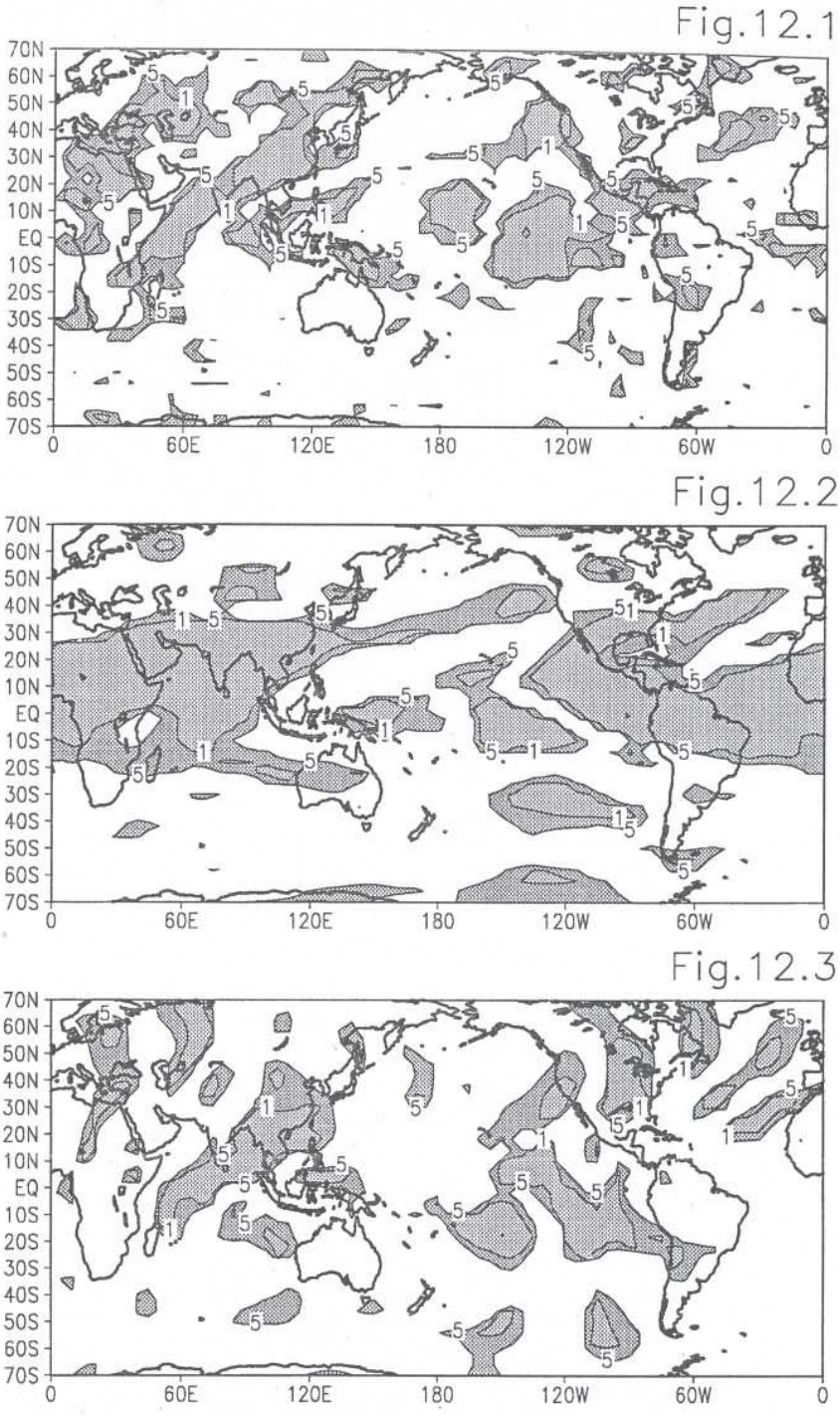

Figure 12. (12.1–12.3) Same as figure 11 except for **C** and **NMA**.

the significance of the GCM simulated summertime anomalies. At each grid point we compute the test statistic

$$t = \frac{\frac{1}{n_1}\sum_{i=1}^{n_1} a_i - \frac{1}{n_2}\sum_{i=1}^{n_2} c_i}{\left(\frac{1}{n_1}+\frac{1}{n_2}\right)^{\frac{1}{2}}\left(\frac{(n_1-1)\sigma_a^2+(n_2-1)\sigma_c^2}{n_1+n_2-2}\right)^{\frac{1}{2}}}, \qquad (1)$$

where a_i is the JJAS mean of any scalar parameter from the ensemble of anomaly runs; c_i is JJAS mean of the corresponding parameter from the ensemble of control runs. Here $n_1 = n_2 = 3$ are the number of ensemble members for the anomaly and control experiments. σ_a and σ_c correspond to standard deviations of the anomaly and control ensembles respectively. The number of degrees of freedom is $(n_1 + n_2 - 2) = 4$. To reject the null hypothesis, that the seasonal mean of a given parameter has not undergone any significant change in the anomaly run relative to the control run, the computed test statistic should exceed the appropriate quantity for any

specified level of significance, which (quantity) can be found from standard tables.

We shall first apply the statistical significance test to the ensemble members of **C** and **E** and identify whether the summer monsoon anomalies induced by the Pacific SST forcing in **E** are statistically significant. Contour maps of significance levels (only 1% and 5% levels) computed from the *t*-test applied to a few parameters (i.e., precipitation and upper level winds) for **C** and **E** are shown in figures (11.1, 11.2 and 11.3). In all the figures, the areas enclosed by the inner contour within the shaded region corresponds to the 1% significance level whereas the areas enclosed by the outer contour corresponds to 5% significance level. It is obvious to see significant changes over the central and eastern Pacific region because of the strong local effect of the SST forcing in **E**. However it is more important to note that the Pacific SST forcing exerts substantial changes over the Indian summer monsoon region as seen from the significance maps of rainfall and wind anomalies. It can be seen that the El Niño induced rainfall changes over northeast India and Head Bay of Bengal, over Arabian Sea and equatorial Indian Ocean are statistically significant. The upper level zonal wind shows substantial changes over northern India in **E** relative to **C**. The upper level meridional winds also show significant changes over north and central India and over the equatorial Indian Ocean.

To assess the statistical significance of the combined effects of the SST forcing and the neglect of orography, we perform the *t*-test for the ensemble members of **C** and **NMA**. Contour maps of significance levels computed from the *t*-test of **C** versus **NMA** are shown in figures 12.1, 12.2 and 12.3. It can be seen that the entire summer monsoon region and large areas in the tropics and extratropics are substantially influenced by the combined effects of SST forcing and the neglect of orography in **NMA**. By comparing figures 11 and 12, it is clear that the neglect of orography in **NMA** has a more dominating influence, over the summer monsoon region and much of the northern extratropics, as compared to the Pacific SST forcing.

8. Dynamical mechanisms

Based on the results of the model simulations, we shall make an attempt to provide a simple conceptual picture of the influence of (**a**) Pacific SST forcing (**b**) Himalayan topography, on the quasi-stationary anomalies over north India.

8.1 *Influence of Pacific SST forcing*

The remote influence of the El Niño forcing on the Indian summer monsoon can occur in two possible ways, viz., (**a**) by modifying the circulations in the tropics (**b**) by modulating the extratropical westerly flow so as to generate cyclonic anomalies over north India.

In the former case, the nearly simultaneous effect of ENSO on the summer monsoon seems to operate directly via., the planetary scale divergent circulations. An anomalous moisture convergence, over the region of the SST anomaly in the equatorial central-eastern Pacific Ocean, gives rise to an anomalous atmospheric heat source locally. This leads to anomalous upward motion over the central-eastern Pacific Ocean and a net sinking motion over the western Pacific Ocean and the monsoon region. In other words, the eastward shift of the Walker cell induced by ENSO affects the low-level moisture convergence field which can in turn influence the monsoon rainfall. In reality it appears that the changes in the divergent circulations actually affect the low-level moisture convergence over the equatorial regions. There is a view that changes in the seasonal mean monsoon precipitation are determined by interactions between convection over the equatorial oceans and the continental convection (see Goswami (1994)). Therefore, it appears that ENSO induced low-level moisture convergence anomalies over the equatorial regions, can affect the bimodality of the oceanic and continental convection zones and thereby produce changes in the monsoon rainfall over the subcontinent.

In the latter case, the effects of the Pacific SST anomaly are indirectly transmitted to the Indian summer monsoon region via., extratropical teleconnections. The influence of the cyclonic anomalies from the extratropics, not only weakens the upper level easterlies and the Tibetan anticyclone but also reduces the north-south thermal contrast due to the incursion of cold and dry air from the high latitudes. A majority of studies in the past have tried to link anomalies in the extratropical wintertime circulations (e.g., Pacific North American (PNA) pattern) and anomalies in tropical convection (see Hoskins and Karoly 1981; Horel and Wallace 1981; Shukla and Wallace 1983). So far there exists two basic theories for explaining the wintertime stationary wave anomalies in the upper troposphere. (**i**) Rossby-wave dispersion on a sphere from a localized tropical heating anomaly and its subsequent interaction with the basic-state flow (Hoskins and Karoly (1981); Webster (1981); Lau and Lim (1984); Sardeshmukh and Hoskins (1988); Rasmusson and Mo (1993)); (**ii**) Generation of fastest growing extratropical normal mode associated with the barotropically unstable basic flow through wave-mean flow interactions (Simmons *et al* (1983); Branstator (1985a)). Both the mechanisms are strongly influenced by the strength and location of the subtropical jet stream during winter. However, it is not clear to what extent these two mechanisms

are viable for the summertime circulations which are characterized by a relatively weak climatological subtropical jet stream that is displaced sufficiently northward over the monsoon region.

The dynamics of the stationary wave anomalies can be clearly illustrated in terms of the forced barotropic vorticity equation given by:

$$\frac{\partial \zeta}{\partial t} + \mathbf{V}\cdot\nabla(\zeta + f) = -(\zeta + f)\nabla\cdot\mathbf{V} + F. \qquad (2)$$

The term $\mathbf{V}\cdot\nabla(\zeta + f)$ in (2) represents the advection of absolute vorticity by the horizontal wind and the term $-(\zeta + f)\nabla\cdot\mathbf{V}$ represents the stretching term and F represents frictional processes. Following Lau and Peng (1992) the variables in (2) can be written as a sum of a time-mean part and a deviation from the time-mean. For instance $\zeta = \bar{\zeta} + \zeta'$, where $\bar{\zeta}$ denotes the time-mean component and ζ' denotes the deviation from the time-mean. The resulting equation can be written in the form:

$$\frac{\partial \zeta'}{\partial t} = A + S + F \quad \text{where} \qquad (3)$$

$$A = -(\bar{\mathbf{V}}_\psi\cdot\nabla\zeta' + \mathbf{V}'_\psi\cdot\nabla\bar{\zeta} + \mathbf{V}'_\psi\cdot\nabla f + \mathbf{V}_{\psi}'\cdot\nabla\zeta').$$

$$S = S1 + S2.$$

$$S1 = -(\bar{\mathbf{V}}_\chi\cdot\nabla\zeta' + \mathbf{V}'_\chi\cdot\nabla\bar{\zeta} + \mathbf{V}'_\chi\cdot\nabla f + \mathbf{V}'_\chi\cdot\nabla\zeta').$$

$$S2 = -(\bar{\zeta}D' + fD' + \zeta'\bar{D} + \zeta'D').$$

In (3) the term A represents vorticity advection by the rotational part of the wind ($\mathbf{V}_\psi$); the term S denotes the source or sink of vorticity anomaly due to the divergent part of the specified winds – which includes the advection ($S1$) and stretching ($S2$) terms due to the divergent winds.

The above equations provide valuable information about the role of tropical heating (divergent) anomalies in inducing anomalous rotational response in the extra-tropics (Sardeshmukh and Hoskins 1988; Krishnan and Mujumdar 1997). Using the model outputs of **C** and **E**, we have computed the different terms in the vorticity equation. The difference (**E-C**) plots of the terms A, $S1$ and S are shown in figures 13.1, 13.2, 13.3 respectively. It is found that the advection of vorticity by the rotational winds (A) is the most dominant term among the three. A similar result was also found by Lau and Peng (1992) and Krishnan and Mujumdar (1997). They pointed out that the relatively minor role played by the $\bar{\mathbf{V}}_\chi$ advection during the northern summer represented a marked deviation of the behaviour as compared to the wintertime circulation (Sardeshmukh and Hoskins (1988)). This may be related to the fact that the climatological subtropical jet stream is relatively weaker and is also shifted much to the north. It can be seen that the term (A) has a wavy pattern that encircles the globe in the extratropics. Although the terms ($S1$) and (S) are smaller when compared to (A), it is nevertheless relevant to note that the effects due to the above two terms are indeed significantly large over India and the neighbourhood. Since the terms $S1$ and S crucially depend on the divergent wind anomalies, we are led to think that the rotational anomalies over north India, during the weak monsoon years, may be basically induced by anomalies in the tropical divergent wind field through the mechanism of Rossby wave dispersion.

Another possibility for the maintenance of the quasi-stationary anomalies is through energy supply from the climatological basic flow via., barotropic process (see Simmons *et al* (1983)). The fact that the stationary wave anomalies have a long persistence, as long as a few months, suggests that the summertime basic flow must have a significant role in internally maintaining the perturbations through constant energy supply. In fact the studies by Branstator (1985b); Blackmon *et al* (1987); and Lau and Peng (1992) suggest that the normal mode mechanism and the mechanism of Rossby wave dispersion are not mutually exclusive but often act in concert to produce large extratropical response initiated by tropical forcing.

8.2 *Influence of the Himalayan topography*

Hahn and Manabe (1975) showed that removal of Himalayas from the GCM leads to a large reduction in the convective heating over the Tibetan plateau and an associated weakening in the intensity of the summer monsoon. In this study, it is found that the Himalayan topography plays an important role in anchoring the El Niño induced extratropical troughs in the high latitudes. From the GCM simulations, it is seen that the neglect of orography favours a southward penetration of anomalous extratropical troughs into the monsoon region. The *mechanical* consequence of these anomalous cyclones is to weaken the upper level easterlies associated with the TEJ and the *thermodynamical* effect is to decrease the monsoon differential heating because of the southward incursion of cold and dry air from the middle latitudes – both of them being adverse to the summer monsoon activity over India.

9. Conclusions

In this paper, ensemble seasonal integrations using the COLA T30L18 GCM were carried out with a view to understand the teleconnection mechanisms through which warm SST anomalies in the equatorial eastern-central Pacific can induce stationary wave anomalies over the Indian summer monsoon region. The role of Himalayan topography in modulating the El Niño induced stationary wave anomalies is also examined in this study. By performing statistical tests on the GCM

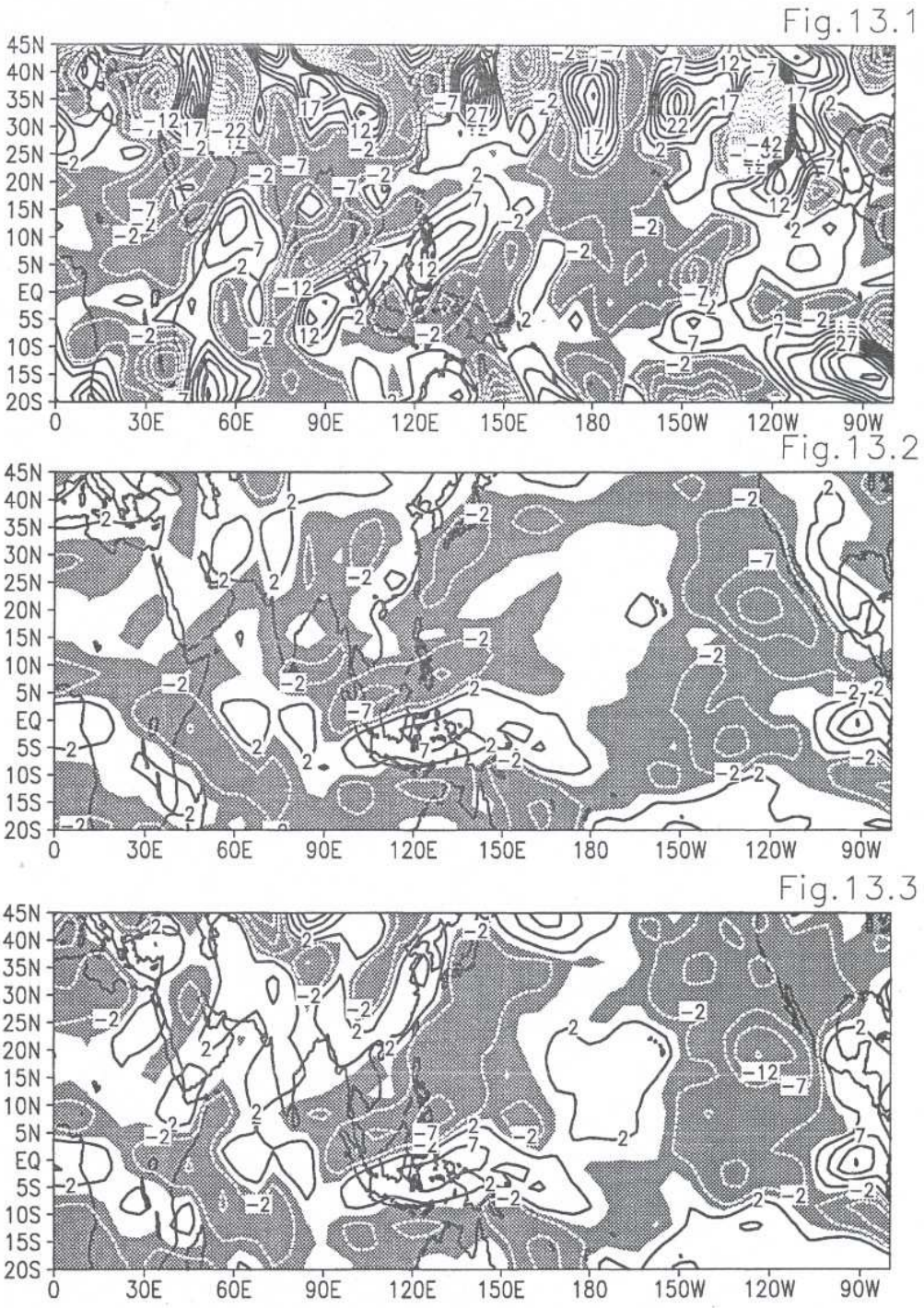

Figure 13. Vorticity generation terms ($\times 10^{-11}\,s^{-2}$) at 200 hPa based on experiments **C** and **E**. (13.1) Term – A; (13.2) Term – $S1$; (13.3) Term – S; Contour interval is 5 units; negative contours are shaded and zero contour is suppressed.

outputs, we have shown that the anomalous effects induced by ENSO and the Himalayan orographic forcing on the stationary wave patterns over the summer monsoon region are indeed statistically significant. The main results of this study are summarized below.

- It is seen that the direct effect of ENSO is to induce major changes in the tropics via., the planetary scale monsoonal divergent circulations leading to modifications of the local Hadley and Walker cells over the Indian monsoon region. These changes in the local Hadley and Walker circulations can affect the moisture convergence and rainfall over the monsoon region. The ENSO induced circulation anomalies over the tropics are associated with larger spatial scales and have a baroclinic structure in the vertical.
- ENSO also affects the Indian summer monsoon indirectly through extratropical teleconnection

anomalies. These mid-latitude effects are transmitted to the monsoon region in the form of anomalous quasi-stationary troughs that can be seen over northwest India and adjoining region during drought years. The extratropical anomalies have a nearly barotropic structure in the vertical and are associated with smaller spatial scales. The influence of the mid-latitude cyclonic anomalies not only weakens the upper level easterlies and the Tibetan anticyclone but also reduces the north-south thermal contrast because of the incursion of cold and dry air from the high latitudes. There seem to be two viable mechanisms by which anomalous tropical convection related with ENSO, can generate stationary wave anomalies over the monsoon region. First is the direct response to Rossby wave dispersion, which is a function of the summertime basic flow. A calculation of the terms in the vorticity equation indicates the possibility of energy being injected into the subtropics by meridionally propagating barotropic Rossby wave trains which emanate from the region of SST forcing. Subsequent interactions between the Rossby wave perturbations and the extratropical westerlies can give rise to quasi-stationary anomalies over the monsoon region. An alternative mechanism is based on the excitation of extratropical normal modes that can extract energy from a zonally varying barotropically unstable basic flow. It is speculated that the latter mechanism can be important for the sustenance of quasi-stationary anomalies which generally have a long persistence.

- Although, the direct and indirect effects of ENSO on the Indian summer monsoon operate separately, it is possible that the individual influence of each of them can act as a positive feedback on the other. For instance, a weakening of the local Walker and Hadley cells, produced by changes in the tropical planetary scale monsoonal divergent circulations, can reduce the monsoon convective activity and weaken the regional scale circulations. The weakening of the regional scale circulations in turn can assist the southward intrusion of cold extratropical westerlies into the monsoon region which further destroys the monsoon activity. In other words there is a possibility that the direct and indirect effects of ENSO on the Indian summer monsoon can go hand in hand.
- GCM simulations with and without orography suggest that the Himalayas play an important role in anchoring the El Niño induced quasi-stationary troughs far to the west in the extratropics. It is found that in the absence of orography the ENSO induced cold extra-tropical cyclonic anomalies tend to intrude southward into the monsoon region; weaken the monsoon differential heating and wipe out the regional scale circulations completely. It is seen that the weakening of the regional scale monsoon circulations due to the neglect of orography is much larger than the weakening induced by the remote ENSO forcing.

Acknowledgements

The authors would like to thank the Director, Indian Institute of Tropical Meteorology, Pune, for providing the necessary facilities to carry out this work. This work has been carried out under the Climate Research Project funded by the Department of Science and Technology (DST), Government of India. We thank Prof. J Shukla and Dr. Mike Fennessy of Center for Ocean-Land-Atmosphere Studies (COLA) for providing us the COLA GCM which was essential for this work. Finally thanks are due to the anonymous referee for suggestions and comments.

List of Abbreviations

CLIM	:	Climatology.
COLA	:	Center for Ocean Land Atmosphere Interactions.
ENSO	:	El Niño - Southern Oscillation.
GCM	:	General Circulation Model.
GFDL	:	Geophysical Fluid Dynamics Laboratory.
IAV	:	Interannual Variability.
ISM	:	Indian Summer Monsoon.
ITCZ	:	Inter Tropical Convergence Zone.
JJAS	:	June, July, August, September.
MONEX	:	Monsoon Experiment.
NCAR	:	National Center for Atmospheric Research.
NCEP	:	National Centers for Environmental Prediction.
NMC	:	National Meteorological Center.
PNA	:	Pacific North American.
SO	:	Southern Oscillation.
SST	:	Sea Surface Temperature.
TEJ	:	Tropical Easterly Jet.
T30L18	:	Triangular Trunctation at 30 Waves and 18 Vertical Levels.

References

Anthes R A 1977 Hurricane model experiments with a new cumulus parameterization scheme; *Mon. Weather. Rev.* **105** 287–300

Banerjee S K 1929 The effect of Indian mountain ranges on the configuration of isobars; *Indian J. Phys.* 4 477–502

Bedi H S, Billa H S and Mukherjee N 1981 Interaction between northern middle latitudes and summer monsoon circulation; *Int. Conf. on early results of FGGE and large scale aspects of its monsoon experiments.* GARP Tallahassee, Florida, 12–17 January 1981, pp 5–25 to 5–29

Bhalme H N and Jadhav S K 1984 The southern oscillation and its relation to the monsoon rainfall; *J. Climatol.* **4** 509–520

Bhalme H N and Mooley D A 1980 Large-scale droughts/floods and monsoon circulation; *Mon. Weather Rev.* **108** 1197–1211

Bjerknes J 1966 A possible response of the atmospheric Hadley circulation to equatorial anomalies of ocean temperature; *Tellus* **18** 820–829

Bjerknes J 1969 Atmospheric teleconnections from the equatorial Pacific; *Mon. Weather Rev.* **97** 163–172

Blackmon M L, Branstator G, Bates G T and Geisler J E 1987 An analysis of equatorial sea surface temperature anomaly experiments in general circulation models with and without mountains; *J. Atmos. Sci.* **44** 1828–1844

Brankovic C, Palmer T N and Ferranti L 1993 Predictability of seasonal atmospheric variations; *J. Climate* **7** 217–237

Branstator G 1985a Analysis of general circulation sea surface temperature anomaly simulation using a linear model. Part I: Forced solutions; *J. Atmos. Sci.* **42** 2225–2241

Branstator G 1985b Analysis of general circulation sea surface temperature anomaly simulation using a linear model. Part II: Eigenanalysis; *J. Atmos. Sci.* **42** 2242–2254

Broccoli A J and Manabe S 1992 The effects of orography on midlatitude northern hemisphere dry climates; *J. Climate.* **5** 1181–1201

Changraney T G 1966 The role of westerly waves in causing flood producing storms over northwest India (excluding Rajastan and Gujarat) during southwest monsoon; *Indian J. Met. Geophy.* **17** 119–126

Chen T C and Yen M C 1994 Interannual variation of the Indian monsoon simulated by the NCAR community climate model: Effect of tropical Pacific SST; *J. Climate* **7** 1403–1415

Chervin R M and Schneider S H 1976 On determining the statistical significance of climate experiments with general circulation models; *J. Atmos. Sci.* **33** 405–412

Fennessy M J, Kinter J L, Kirtman B, Marx L, Nigam S, Schneider E, Shukla J, Vernekar A, Xue Y and Zhou J 1994 The simulated Indian monsoon. A GCM sensitivity study; *J. Climate* **7** 33–43

Gadgil S 1977 Orographic effect on the southwest monsoon – a review; *Pure Appld. Geophys.* **115** 1413–1430

Gilchrist A 1977 The simulation of the Asian Summer Monsoon; *Pure Appld. Geophys.* **115** 1431–1448

Gill A E 1980 Some simple solutions for heat induced tropical circulation; *Q. J. R. Meteorol. Soc.* **106** 447–463

Godbole R V 1973 Numerical simulation of the Indian summer monsoon; *Indian J. Meteorol. Geophys.* **24** 1–14

Goswami B N 1994 Dynamical predictability of seasonal monsoon rainfall. Problems and prospects; *Proc. Indian Natl. Acad. Sci.* **60A** 101–120

Hahn D G and Manabe S 1975 The role of mountains in the south Asian monsoon circulation; *J. Atmos. Sci.* **32** 1515–1541

Harshvardhan, Davis R, Randall D A and Corsetti T G 1987 A fast radiation parameterization for general circulation models; *J. Geophys. Res.* **92** 1000–1016

Holton J R 1979 An introduction to Dynamic Meteorology; Academic Press, pp 89–90

Horel J D 1981 A rotated principal component analysis of the interannual variability of the northern hemisphere 500 mb height field; *Mon. Weather Rev.* **109** 2080–2092

Horel J D and Wallace J M 1981 Planetary scale atmospheric phenomena associated with the Southern Oscillation; *Mon. Weather Rev.* **109** 813–829

Hoskins B J and Karoly D J 1981 The steady linear response of spherical atmosphere to thermal and orographical forcing; *J. Atmos. Sci.* **38** 1179–1196

Joseph P V 1978 Sub-tropical westerlies in relation to large scale failure of Indian monsoon; *Indian J. Met. Hydrol. Geophys.* **29** 412–418

Joseph P V, Mukhopadhyaya R K, Dixit N V and Vaidya D V 1981 Meridional wind index for long range forecasting of Indian summer monsoon rainfall; *Mausam* **32** 31–34

Ju J and Slingo J 1995 The Asian summer monsoon and ENSO; *Q. J. R. Meteorol. Soc.* **121** 1133–1168

Kalnay E, Kanamitsu M, Kistler R, Collins W, Deaven W, Gandin L, Iredell M, Saha S, White G, Woollen J, Zhu Y, Chelliah M, Ebisuzaki W, Higgins W, Janowiak J, Mo K C, Ropelewski C, Wang J, Leetmaa A, Reynolds R, Roy Jenne and Dennis Joseph 1996 The NCEP/NCAR 40-Year Reanalysis Project; *Bull. Amer. Meteorol. Soc.* **77** 437–471

Kanamitsu M, Krishnamurti T N and Depradine C 1972 On scale interaction in the tropics during northern summer; *J. Atmos. Sci.* **29** 698–706

Kanamitsu M and Krishnamurti T N 1978 Northern summer tropical circulations during drought and normal rainfall months; *Mon. Weather Rev.* **106** 331–347

Keshavamurty R N 1982 Response of the atmosphere to sea surface temperature anomalies over the equatorial Pacific and teleconnection of the southern oscillation; *J. Atmos. Sci.* **39** 1241–1259

Keshavamurty R N and Awade S T 1974 Dynamical abnormalities associated with drought in the Asiatic summer monsoon; *Indian J. Met. Geophysics* **25** 257–266

Keshavamurty R N, Satyan V, Dash S K and Sinha H S S 1980 Shift of quasi-stationary features during active and break monsoons; *Proc. Indian Acad. Sci., (Earth Planet. Sci.)* **97** 127–136

Kiladis G N and Diaz H F 1989 Global climatic anomalies associated with extremes in the Southern Oscillation; *J. Climate.* **2** 1069–1090

Krishnamurti T N 1971a Tropical east-west circulations during the northern summer; *J. Atmos. Sci.* **28** 1342–1347

Krishnamurti T N 1971b Observational study of the tropical upper tropospheric motion field during the northern hemispheric summer; *J. Appl. Meteor.* **10** 1066–1096

Krishnamurti T N, Bedi H S and Subramaniam M 1989 The summer monsoon of 1987; *J. Climate.* **2** 321–340

Krishnamurti T N, Bedi H S and Subramaniam M 1990 The summer monsoon of 1988; *Met. Atmos. Phys.* **42** 19–37

Krishnamurti T N, Daggupaty S M, Fein J, Kanamitsu M and Lee J D 1973 Tibetan high and upper tropospheric tropical circulations during northern summer; *Bull. Amer. Meteorol. Soc.* **54** 1234–1249

Krishnamurti T N and Surgi N 1987 Observational aspects of summer monsoon; *Monsoon Meteorology* (ed.) C P Chang and T N Krishnamurti Oxford University Press, 3–25

Krishnan R and Fennessy M J 1997 GCM simulations of intraseasonal variability in the Indian summer monsoon; *Tech. Rep. No. 40, Center for Ocean Land Atmosphere Interactions (COLA), USA*

Krishnan R and Mujumdar M 1997 Regionally and remotely forced premonsoon signals over northern India and neighbourhood; *Q. J. R. Meteorol. Soc.* (under revision)

Kuo H L 1965 On the formation and intensification of tropical cyclones through latent heat release by cumulus convection; *J. Atmos. Sci.* **22** 40–63

Lacis A A and Hansen J E 1974 A parameterization for the absorption of solar radiation in the earth's atmosphere; *J. Atmos. Sci.* **31** 118–133

Lau K M and Lim H 1984 On the dynamics of equatorial forcing and climate teleconnections; *J. Atmos. Sci.* **41** 161–176

Lau K M and Peng L 1992 Dynamics of atmospheric teleconnections during the northern summer; *J. Climate* **5** 140–158

Lau K M and Sheu P J 1988 Annual cycle, quasi-biennial oscillation and southern oscillation in global precipitation; *J. Geophys. Res.* **93** 10975–10988

Matsuno T 1966 Quasi-geostrophic motions in the equatorial area; *J. Meteorol. Soc. Japan* **44** 25–43

Mellor G L and Yamada T 1982 Development of a turbulence closure model for geophysical fluid problems; *Rev. Geophys. Space Phys.* **20** 851–875

Miller M J, Beljaars A C M and Palmer T N 1992 The sensitivity of the ECMWF model to the parameterization of evaporation from the tropical oceans; *J. Climate* **5** 418–434

Mooley D A 1957 The role of western disturbances in the production of weather over India during different seasons; *Indian J. Met. Geophy.* **8** 253–260

Murakami T 1974 Steady and transient waves excited by diabatic heat sources during the summer monsoon; *J. Atmos. Sci.* **31** 340–357

Nigam S 1994 On the dynamical basis for the Asian summer monsoon Rainfall-El Niño relationship; *J. Climate* **7** 1750–1771

Palmer T N, Brankovic C, Viterbo P and Miller M J 1992 Modelling interannual variations of summer monsoons; *J. Climate* **5** 399–417

Pan H-L 1979 Upper tropospheric tropical circulations during a recent decade; *Report No. 79–1, Department of Meteorology*, Florida State University, Tallahassee, Florida

Pant G B and Parthasarthy B 1981 Some aspects of an association between the Southern Oscillation and Indian summer monsoons; *Arch. Meteor. Geophys. Biokl.* **B29** 245–252

Parthasarathy B, Diaz H F and Eischeid J K 1988 Prediction of all-India summer monsoon rainfall with regional and large-scale parameters; *J. Geophys. Res.* **93** D5 5341–5350

Parthasarathy B, Munot A A and Kothawale D R 1995 Monthly and seasonal rainfall series for All-India homogenous regions and meteorological subdivisions: 1871–1994; *Research Report No. RR-065*, Indian Institute of Tropical Meteorology, Pune, India

Pisharoty P R and Desai B N 1956 Western disturbances and Indian weather; *Indian. J. Met. Geophys.* **7** 4 333–338

Rajeevan M 1991 Upper air circulation and thermal anomalies over India and neighbourhood vis-a-vis Indian summer monsoon activity; *Mausam* **42** 155–160

Rajeevan M 1993 Upper tropospheric circulation and thermal anomalies over central Asia associated with major drought and floods in India; *Curr. Sci.* **64** 244–247

Ramamurthy K 1969 Some aspects of 'break' in the Indian southwest monsoon during July and August; *Forecasting manual*, Indian Meteorological Department Publication, FMU, Rep. 4, 18.3

Raman C R V and Rao Y P 1981 Blocking highs over Asia and monsoon droughts over India; *Nature* **289** 221–223

Ramaswamy C 1958 A preliminary study of the behaviour of the Indian southwest monsoon in relation to the westerly jet stream; *Geophysica* **6** 455–476

Ramaswamy C 1962 Breaks in the Indian summer monsoon as a phenomenon of interaction between the easterly and subtropical westerly jet streams; *Tellus* **14** 337–349

Rasmusson E M and Carpenter T H 1983 The relationship between eastern equatorial Pacific sea surface temperature and rainfall over India and Sri Lanka; *Mon. Weather Rev.* **111** 517–528

Rasmusson E M and Mo K-C 1993 Linkages between 200-mb tropical and extratropical anomalies during the 1986–1989 ENSO cycle; *J. Climate* **6** 595–616

Rasmusson E M and Wallace J M 1983 Meteorological aspects of the El Niño/Southern Oscillation; *Science* **222** 1195–1202

Reynolds R W and Smith T M 1994 Improved global sea surface temperature analyses using optimum interpolation; *J. Climate* **7** 929–948

Ropelewski C F and Halpert M S 1987 Global and regional scale precipitation patterns association with El Niño/Southern Oscillation; *Mon. Weather Rev.* **115** 1606–1626

Rowntree P R 1972 The influence of tropical east Pacific Ocean temperature on the atmosphere; *Q. J. R. Meteorol. Soc.* **98** 290–321

Sardeshmukh P D and Hoskins B J 1988 The generation of global rotational flow by steady idealized tropical divergence; *J. Atmos. Sci.* **40** 1228–1251

Sarkar R P 1966 A dynamical model of orographic rainfall; *Mon. Weather Rev.* **94** 555–572

Schemm J, Schubert S, Terry J and Bloom S 1992 Estimates of monthly mean soil moisture for 1979–1989; NASA Tech. Mem. 104571, October 1992, Goddard Space Flight Center, Greenbelt, MD 20771

Sela J G 1982 The NMC spectral model; NMC Office Note 30, U.S. Department of Commerce, NOAA, NWS, 36 pp

Shukla J 1975 Effect of Arabian sea-surface temperature anomaly on Indian summer monsoon. A numerical experiment with the GFDL model; *J. Atmos. Sci.* **32** 503–511

Shukla J and Fennessy M J 1994 Simulation and predictability of Monsoons; *Proc. International Conference on Monsoon Variability and Prediction*, ICTP, Trieste, WMO/TD-No.619. 567–575

Shukla J and Paolino D A 1983 The Southern Oscillation and long range forecasting of the summer monsoon rainfall over India; *Mon. Weather Rev.* **111** 1830–1837

Shukla J and Wallace J M 1983 Numerical simulation of the atmospheric response to equatorial Pacific sea surface temperature anomalies; *J. Atmos. Sci.* **40** 1613–1630

Sikka D R 1980 Some aspects of the large-scale fluctuations of summer monsoon rainfall over India in relation to fluctuations in planetary and regional scale circulation parameters; *Proc. Indian Acad. Sci. (Earth Planet. Sci.)* **89** 179–195

Sikka D R and Grossman H 1981 Large scale features associated with the evolution and intensification of the break monsoon over India during August 1979; Florida MONEX Conference, 1–67 to 1–70

Simmons A J, Wallace J M and Branstator G 1983 Barotropic wave propagation and instability and atmospheric teleconnection patterns; *J. Atmos. Sci.* **40** 1363–1392

Simpson G C 1921 The southwest monsoon; *Q. J. R. Met. Soc.* **47** 151–172

Spangler W M and Jenne R L 1990 World monthly surface station climatology; National Center for Atmospheric Research, Boulder, CO 80303

Spencer R W 1993 Global oceanic precipitation from the MSU during 1979–91 and comparisons to other climatologies; *J. Climate* **6** 1301–1326

Sperber K R, Hameed S, Potter G L and Boyle J S 1994 Simulation of the northern summer monsoon in the ECMWF model: Sensitivity to horizontal resolution; *Mon. Weather Rev.* **122** 2461–2481

Stoeckenius T 1981 Interannual variations of tropical precipitation patterns; *Mon. Weather Rev.* **109** 1233–1247

Sud Y C and Walker G K 1992 A review of recent research on improvement of physical parameterizations in the GLA GCM Physical Processes in Atmospheric Models; (eds) D R Sikka and S S Singh, Wiley Eastern 424–479

Tiedke M 1984 The effect of penetrative cumulus convection on large scale flow in a general circulation model; *Beitr. Phys. Atmos.* **57** 216–239

Ting M 1994 Maintenance of northern summer stationary waves in a General Circulation Model; *J. Atmos. Sci.* **51** 3286–3308

Unni Nayar M S and Murakami T 1978 Temporal variations in the northern hemispheric summer circulations; *Indian J. Met. Geophy.* **29** 1 170–186

Van Loon H and Madden R A 1981 The Southern Oscillation. Part I: Global associations with pressure and temperature in northern winter; *Mon. Weather Rev.* **109** 1150–1162

Verma R K 1982 Long range prediction of monsoon activity: A synoptic diagnostic study; *Mausam* **33** 35–44

Wallace J M and Gutzler D S 1981 Teleconnections in the geopotential height field during the northern hemisphere winter; *Mon. Weather Rev.* **109** 785–812

Washington W M, Chervin R M and Rao G V 1977 Effects of a variety of Indian Ocean surface temperature anomaly patterns on the summer monson circulation: Experiments with the NCAR General Circulation Model; *Pure Appld. Geophys.* **115** 1335–1356

Webster P J 1981 Mechanisms determining atmospheric response to sea surface temperature anomalies; *J. Atmos. Sci.* **38** 554–571

Webster P J 1972 Response to tropical atmosphere to local, steady forcing; *Mon. Weather Rev.* **100** 518–541

Webster P J and Yang S 1992 Monsoon and ENSO: Selectively interactive systems; *Q. J. R. Meteorol. Soc.* **118** 877–926

White G 1982 An observational study of the northern hemisphere extratropical summertime general circulation; *J. Atmos. Sci.* **39** 24–40

Wright P B 1977 The southern oscillation, patterns and the mechanisms of teleconnections and persistence; *Hawaii Institute of Geophysics*, Univ. of Hawaii, HIG–79–13, 107 pp

Xue Y, Sellers P J, Kinter J and Shukla J 1991 A simplified biosphere model for global climate studies; *J. Climate* **4** 345–364

Zwiers F W 1993 Simulation of the Asian summer monsoon with the CCC GCM-1; *J. Climate* **6** 470–486